INTERACTIONS OF METAL CATIONS WITH DNA MONOLAYERS: BINDING KINETICS AND SENSING APPLICATIONS

by

Li Su
B. Sc., Shandong University, 2001

THESIS SUBMITTED IN PARTIAL FULFILLMENT OF
THE REQUIREMENTS FOR THE DEGREE OF

MASTER OF SCIENCE

In the Department of Chemistry

SIMON FRASER UNIVERSITY

Fall 2004

SIMON FRASER UNIVERSITY

Partial Copyright Licence

ABSTRACT

Electrostatic interactions with metal ions are essential to the structural stability and polymorphism of oligonucleotides. This thesis describes the extended applications of a simple electrochemical protocol, based on the voltammetric response of multiply-charged transition metal cations ($[Ru(NH_3)_6]^{3+}$) bound electrostatically to DNA- modified surfaces, to explore the kinetics of metal ion-DNA interactions and potential sensing applications of DNA-modified electrodes.

We first analyzed the time-dependent voltammetric behavior of the redox cation $[Ru(NH_3)_6]^{3+}$ binding to and dissociating from thiolate-DNA monolayers on gold. It was found that the ion-exchange binding kinetics is dominated by the structure of the DNA monolayers, i.e., the apparent first-order rate constant decreases significantly upon increasing the surface density of DNA strands. Furthermore, it has been shown that second-order binding rate constants can be derived from the dependence of the apparent first-order rate constants on the solution concentration of the redox cations, and the dissociation rate constants were obtained by transferring the incubated electrode into a buffer solution free of redox cations.

The research was then extended to the potential sensing applications of DNA-modified electrodes. After incubation in a dilute solution of redox transition metal cations, the DNA-modified electrode responds to non-electroactive metal ions, particularly those are important in biological systems. Magnesium, calcium and potassium can be detected at very low concentration levels (micromolar), and that the sensitivity decreases

significantly for the monocations (e.g., K^+). The derived equilibrium binding constants of the divalent metal cations to DNA-modified electrodes confirm that Mg^{2+} is binds more strongly to DNA than Ca^{2+}.

The last part of this thesis describes our first attempt to develop a chip-based electrochemical deoxyribosensor, for which we incorporated a specific nucleic acid adapter (so-called "aptamer") for ATP and adenosine into DNA monolayers on gold. The binding of molecular analytes (e.g., adenosine) induces a conformational change that can be revealed by the voltammetric response of electrostatically bound redox cations: a clear increase of the integrated charge is observed upon increasing the concentration of adenosine in solution. We have also determined the binding constant of adenosine to the deoxyribosensor based on a simple Langmuir model.

DEDICATION

献给我深爱的父母: 爸爸苏有前, 妈妈张西华,及未婚夫秦晋.

谢谢您们的支持,关心与爱!

This thesis is dedicated to

my beloved parents, Youqian Su and Xihua Zhang,

my fully supporting fiancé, Jin Qin.

Thanks for your love, support and patience!

ACKNOWLEDGEMENTS

I would like to express my sincere gratitude to my senior supervisor, Dr. Hua-Zhong (Hogan) Yu. Thanks for his guidance, encouragement, and patience throughout my degree. His great enthusiasm and integral view on research has made a deep impression on me. I'll benefit from his attitude in my whole life.

I would like to thank my co-supervisor, Dr. Dipankar Sen and my supervisory committee members, Dr. Paul Li and Dr. Ross Hill for their helpful suggestions and advice.

I would also like to thank Dr. Melanie O'Neill for being my internal examiner.

I would like to thank the following for their contributions to this thesis. Chuan-Yun Luo for her experience and training when I was starting to do my project. Carlo Sankar in Dr. Sen's lab for helping with the preparation of DNA samples. Dr. Eberhard Kiehlmann for proofreading my thesis and helpful suggestions.

All members of Dr.Yu's lab for their friendship and helpful discussions.

TABLE OF CONTENTS

LIST OF FIGURES

LIST OF TABLES

LIST OF ABBREVIATIONS AND SYMBOLS

AQ	Anthraquinone
ATP	Adenosine Triphosphate
A-T	Adenine and Thymine
bipy	Bipyridine
C-G	Guanine and Cytosine
C_{Ru}	Concentration of $[Ru(NH_3)_6]^{3+}$ in solution
CV	Cyclic Voltammetry
DMT	Dimethoxytrityl
DNA	Deoxyribonucleic Acid
dsDNA/Au	Double Stranded DNA Modified Gold Surfaces
DTT	Dithiothreitol
Γ_{DNA}	Surface Density of DNA
Γ_{Ru}	Surface Concentration of $[Ru(NH_3)_6]^{3+}$
LB	Leucomethylene Blue
MB	Methylene Blue
MCH	6-Mercapto-1-hexanol
Q	Integrated Charge of Surface-bound $[Ru(NH_3)_6]^{3+}$

SAM	Self-Assembled Monolayer
ssDNA/Au	Single Stranded DNA Modified Gold Surfaces
θ	Surface Coverage
Tris	N-tris [hydroxymethyl] aminomethane

CHAPTER 1
GENERAL INTRODUCTION

In this thesis, kinetics of metal ion-DNA interaction on surfaces and sensing applications of DNA-modified electrodes are explored by simple electrochemical methods. As a general introduction of the background for this research, the following sections will briefly describe the structure and properties of DNA (to show the molecular principles behind DNA sensing technology), DNA sensing technology (particularly DNA microarrays), DNA surface chemistry (to address the conformation and reactivity of DNA on surfaces), metal ion-DNA interactions, and previous work (including introductions of cyclic voltammetry and the Langmuir model), respectively.

1.1 DNA Structure and Properties

DNA (deoxyribonucleic acid) is the major component of chromosomes and carries genetic information for making living organisms.[1a] In the past few decades, DNA chemistry has triggered research advances in almost all fields of life sciences, which opened up new opportunities for the investigation of molecular details of eukaryotic gene structure and function. The molecular principles behind the gene technology, including DNA hybridization, amplification, and recombination, are all based on the double helical structure of DNA molecules, which was first discovered by Watson and Crick in 1953.[2] The complementary nature of the base pairing between adenine and thymine (A-T) as well as guanine and cytosine (G-C) (Figure 1-1) is the basis for the replication of DNA double helices and also makes DNA particularly well suited for biosensing applications.

Typically the DNA double helix is stabilized by hydrogen bonding and base stacking interactions, as mentioned above (Figure 1-1).

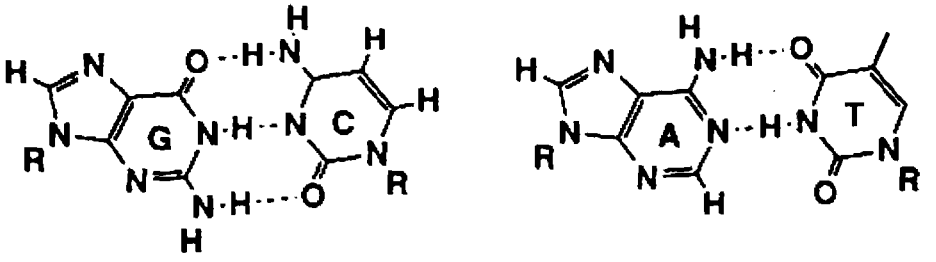

Figure 1-1 Watson-Crick base pairing in DNA. A: adenine; C: cytosine; G: guanine; T: thymine.

The structure of DNA is illustrated by a double helix (think of a spiral staircase), with 10 nucleotide pairs per helical turn (for B-DNA).[1b] Each spiral strand, comprised of a sugar-phosphate backbone and attached bases, is connected to a complementary strand by hydrogen bonding between paired bases. The sugar-phosphate backbone is on the outside of the helix where the polar phosphate groups can interact with the polar environment. The nitrogen-containing bases are inside, stacking perpendicular to the helix axis. Figure 1-2 shows one portion of the DNA double helix with details of how the bases, sugars, and phosphates connect to form the structure of the molecule.

At neutral, physiological pH, each phosphate group of the backbone carries a negative charge. Positively charged ions such as Na^+ or Mg^{2+} and polypeptides with positively charged side chains are frequently associated with DNA as a result of electrostatic attraction (as described in the following sections).[1b]

There are three types of DNA double helices, i.e., A-type, B-type, and Z-type. The right-handed B-type helix is the typical structure under conditions of neutral pH and moderate (physiological) salt concentrations. The B-type double helix is relatively

sequence-independent, i.e., all DNA sequences can form it if the appropriate complementary sequence is available. An A-type helix is typical when DNA is hybridized to RNA. Compared to the B-type and A-type helix, the Z-type is left-handed and requires specific sequences such as alternating GC repeats as well as relatively high salt concentrations.[1b]

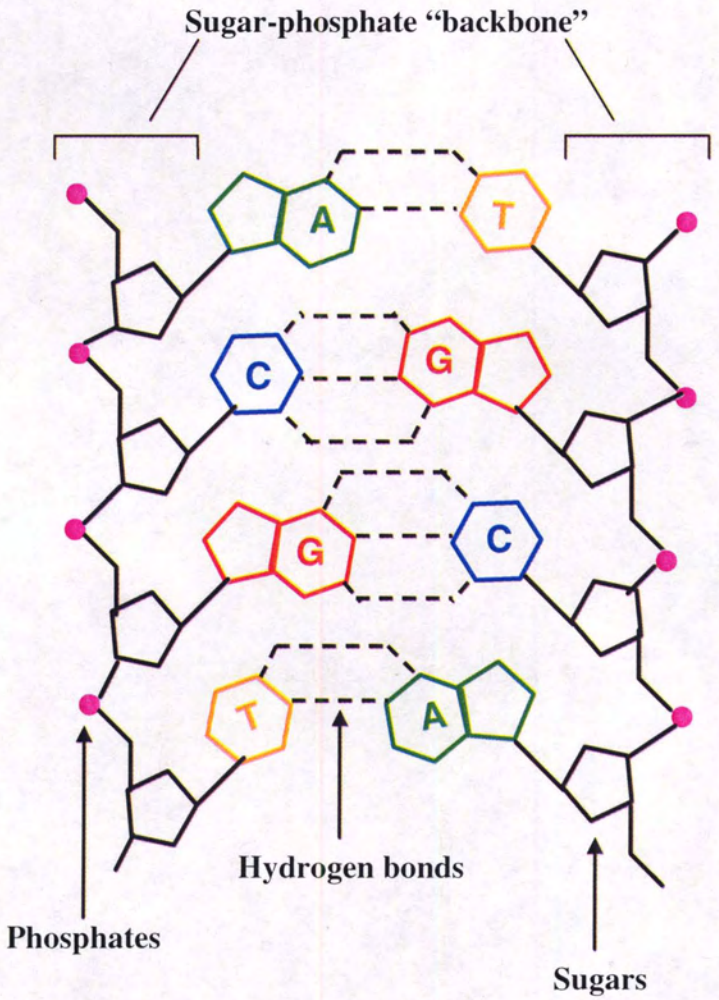

Figure 1-2 **Schematic representation of DNA structure along with details of the connections between bases, sugars, and phosphates.**

1.2 DNA Sensing Technology: DNA Microarrays

Sequencing of DNA samples, detection of DNA damage, and investigation of DNA interactions with other molecules are currently exploited as the central themes of the DNA-based biosensing technology. Its potential applications include gene discovery, disease diagnosis, drug discovery, and toxicological research.[3]

In recent years, large scale DNA testing has made the conventional detection methods inadequate to meet the requirement of developing small, fast and easy-to-use analytical devices. DNA microarrays (also called gene chips, DNA chips, or biochips) offer attractive features: miniaturization, speed, and accuracy. Typically, DNA microarrays are prepared by using photolithographic methods, which are more commonly used for integrated circuit (computer chip) production. Hence the colloquial term "DNA chip" came into being.[4]

DNA microarrays are typically monolithic, flat surfaces that bear multiple, high-density single-stranded oligonucleotide sequences. These probes are used to detect complementary DNA fragments by imaging technologies, most often fluorescence or radioisotopic detection.[4a] Traditional methods in molecular biology generally work on a "one gene in one experiment" basis, which means that the throughput is very limited and the "whole picture" of gene function is difficult to obtain. The DNA microarray technology promises to monitor the whole genome on a single chip so that researchers can have a better picture of the interactions among thousands of genes simultaneously. For example, Affymetrix (Santa Clara, CA) can produce the gene chip that is packed with fragments from each of the approximately 35,000 known genes that make up the human genome.[5] The company also sells a number of GeneChips for screening for breast cancer,

detecting mutations in the HIV genome and in the *p53* tumor-supressor gene, and identifying bacterial pathogens.[4c, 5]

However, traditional DNA chips are normally based on optical detection, which requires highly precise and expensive instrumentation as well as sophisticated numerical algorithms to interpret the data.[6] During the last decade, continued efforts have been made to search for ideal substrates, optimal synthetic routes, and sensitive detection methods for DNA chips. Many branches of chemistry have contributed to the improvement of DNA microarray techniques; for example, synthetic chemistry helps to attach probe strands or prepare DNA samples, physical chemistry to characterize the structure of DNA layers on surfaces, and analytical chemistry to assess surface reactions.[4a] The microarrays can be prepared on the surfaces of glass slides, polymer substrates, carbon, gold, or silicon. There are mainly two methods for fabricating the DNA probe arrays on a substrate.[7] One is the direct on-surface synthesis of oligonucleotides;[8] the other is the attachment of pre-synthesized oligonucleotides that are chemically modified for covalent immobilization on substrates.[9] The latter method is more common due to the simpler procedure and least requirements of facilities.

1.3 DNA Surface Chemistry

As microarray technology continues to emerge as an alternative to conventional DNA diagnostic methods, questions about the conformation and reactivity of DNA probes on surfaces must be addressed.[7] Depending on the nature of the substrate, various schemes can be used for attaching DNA probes to the surface. Common immobilization strategies include the attachment of biotin-functionalized DNA probes to avidin-coated surfaces, self-assembly of thiol-tethered DNA probes onto gold substrates, and covalent

(carbodiimide) coupling to hydroxyl groups on carbon electrodes.[10] Thiolate-DNA monolayers on gold are of great interest because of their simple preparation and versatility for molecular modifications; they are suitable model systems for fundamental studies of DNA surface chemistry.[11]

1.3.1 Thiolate-DNA Monolayers on Gold and Their Characterization

Self-assembly is one of the ubiquitous events in chemical and biological processes. In a self-assembled monolayer (SAM) formed on solid surface, the molecules exhibit a high degree of orientation, order, and packing. Gold is the most popular substrate to prepare SAMs by adsorption of n-alkanethiols and their derivatives. Owing to its noble character, gold does not form a stable oxide surface layer, and can survive harsh chemical treatments for cleaning. The strong sulfur-gold interaction makes these monolayers relatively stable in air and in electrolyte.[12]

Similar to long-chain n-alkanethiols, thiol-tethered DNA single or double strands (for certain lengths only) form uniform and closely packed monolayers on gold surface. The effect of length and the presence of an anchoring group on the assembly of DNA single strands on gold surface have been studied previously.[7] The investigation is based on the immobilization of single-stranded oligonucleotides containing a 5'-hexanethiol anchoring group for lengths from 8 to 48 bases. It has been shown that the thiol group strongly enhances oligonuleotide immobilization, but the enhancement is reduced for longer strand lengths. For strands longer than 24 bases, the surface coverage begins to decrease noticeably. The decrease is consistent with a less ordered arrangement of the DNA chains, presumably reflecting increasing polymeric behavior.[7] To improve the quality, gold substrates modified with DNA monolayers are normally treated with dilute

solutions of 6-mercapto-1-hexanol (MCH). The strong affinity of the thiol group of MCH for gold results in the displacement of less strongly, non-specifically adsorbed DNA bases. The net negative dipole of the alcohol terminus repels the negatively charged DNA backbone, thus helping to project the DNA strands into solution (see Figure 1-4).[11a, 13]

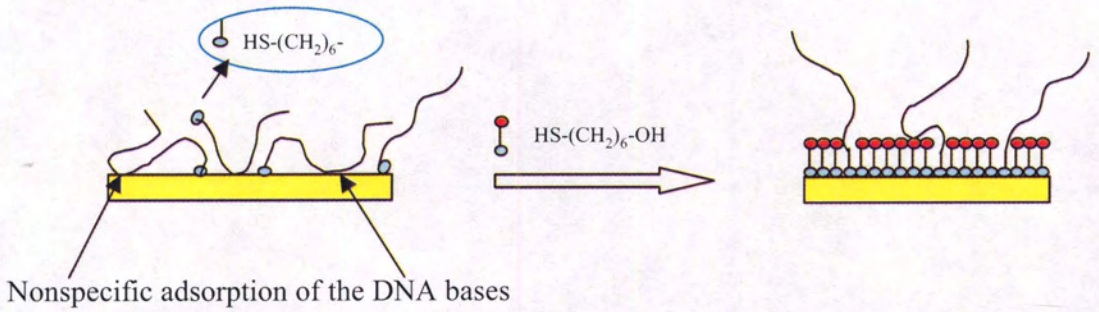

Figure 1-3 Cartoon drawing of the formation of thiolate DNA monolayers on gold: before and after treatment with MCH.

Various techniques have been employed to characterize DNA monolayers on gold, including surface plasmon resonance spectroscopy, neutron reflectivity, scanning force microscopy, ^{32}P-radiolabeling, ellipsometry, X-ray photoelectron spectroscopy, infrared spectroscopy, and fluorescence-based methods.[11a, 13a, 14] For example, the neutron reflectivity studies have indicated that single-stranded DNA adsorbs to gold via multiple amine moieties, as amines are known to chemisorb weakly to gold surfaces.[13a] X-ray photoelectron spectroscopy, ellipsometry, and ^{32}P-radiolabeling experiments indicated that the non-specific adsorption of DNA bases can be prevented by treating the thiolate-DNA monolayer modified gold substrates with dilute solutions of 6-mercapto-1-hexanol (MCH).[11a] The detection of hybridization and denaturation of thiol-thethered DNA using two-color surface plasmon resonance spectroscopy was developed by Tarlov et. al.[14a]

Recently, the use of colloidal gold particles as topographic labels to characterize DNA hybridization on gold substrates by scanning force microscopy was proposed by Fritzsche and co-workers,[14b] which opens an avenue to characterize DNA monolayers on gold with a lateral resolution in the nanometer range. However, these methods cannot satisfy the requirement of developing easy-to-use, fast, inexpensive, miniaturized analytical devices for wide-scale genetic testing requirements. Electrochemical approaches promise to provide a simple, accurate, and inexpensive alternative for DNA diagnosis.

1.3.2 Electrochemical Study of DNA Modified Surfaces

Palecek and co-workers pioneered the electrochemical detection of nucleic acids.[15] They found that the nucleobases were electroactive when adsorbed to mercury or carbon electrodes. Thereafter, tremendous efforts have been devoted to the detection of nucleic acids using DNA-modified solid electrodes, which represent the basis of electrochemical DNA sensors. Key technological advances in this field have been summarized in several recent review articles;[6, 16] many practical approaches have been explored to develop electrochemical methods to study DNA-modified surfaces, including label-free and redox labels-based detections as outlined below.

1.3.2.1 Label-Free Electrochemical Detection

Label-free electrochemical detection schemes are based on direct or catalyzed oxidation of DNA bases. Among the four nucleic acid bases, the oxidation of guanine (G) moiety is the easiest.[6] Adsorption stripping voltammetry was one of the typical electrochemical techniques to detect DNA oxidation directly.[17] It offers high selectivity, but significant background currents at the required relatively high potentials complicate

its application. Some recent designs employ physical separation techniques to remove the sources of this background interference.[18]

Oxidation of target DNA catalyzed by redox mediators, such as $Ru(bipy)_3^{2+}$, have been proposed recently.[19] As shown in Figure 1-4, the guanine residues reduce the metal

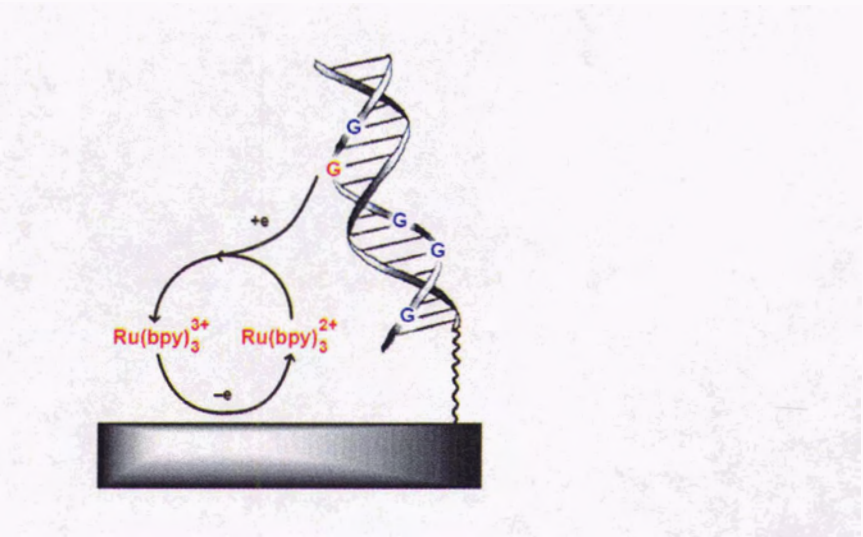

Figure 1-4 Schematic representation of guanine oxidation mediated by a ruthenium complex in solution [Adapted by permission. Ref. 6] It should be noted that the author is using the abbrivation of bpy for bipyridine instead of bipy that is more common. In addition, the left one should be $Ru(bpy)_3^{2+}$, while the right one should be $Ru(bipy)_3^{3+}$.

complex that subsequently diffuses to the electrode surface where it is re-oxidized. The catalytic cycle is represented by equations (1) and (2):

$$Ru(bipy)_3^{3+} + G \rightarrow Ru(bipy)_3^{2+} + G^+ \qquad (1)$$

$$Ru(bipy)_3^{2+} \rightarrow Ru(bipy)_3^{3+} + e^- \qquad (2)$$

The enhanced signal reflects the amount of guanine available for oxidation.

1.3.2.2 Redox Label-Based Detection

Early work focused on using redox indicators to differentiate between single and double strands of DNA on the electrode surface. Mikkelsen and co-workers demonstrated about a decade ago that immobilized DNA (on activated glassy carbon electrodes) can be detected voltammetrically using redox indicators ($[Co(bipy)_3]^{3+}$ and $[Co(phen)_3]^{3+}$), which bound to DNA electrostatically.[20] Tarlov and co-workers showed that by using a chronocoulometric scheme, DNA hybridization on thiolate-DNA-modified gold surfaces could be easily detected based on the response of multiply charged redox cations bound electrostatically to DNA strands on the surface. The amount of DNA strands present on the electrode surface can be determined from the integrated charge of the surface redox reaction.[21] As further demonstrated in this thesis, electrostatic probe molecules binding to DNA immobilized surfaces can be used to design various DNA sensors as well as to study fundamental and practical aspects of metal ion-DNA interactions.

When using a redox-active intercalator, such as methylene blue (MB) or daunomycin, the redox species is oxidized and reduced respectively via DNA-mediated long-range electron transfer. Barton and colleagues reported that by using MB as an intercalator and potassium ferricyanide as an electrocatalyst,[6, 22] single-base mismatches could be detected based on the efficiency of electron transfer through DNA double helices. Figure 1-6 shows the electrochemical assay for mismatches through DNA-mediated electron transfer experiments. On the right is shown an electrode modified with well-matched duplex DNA. Current flows through the DNA to reduce methylene blue (MB^+), intercalated near the top of the DNA monolayer, to leucomethylene blue (LB). LB goes on to reduce ferricyanide in solution, thereby regenerating MB^+ catalytically,

leading to an amplification of the hybridization signal. In the case of a DNA monolayer containing mismatched duplexes (left), current flow through the DNA duplex is attenuated, MB^+ cannot be reduced, and the catalytic signal is lost.[6]

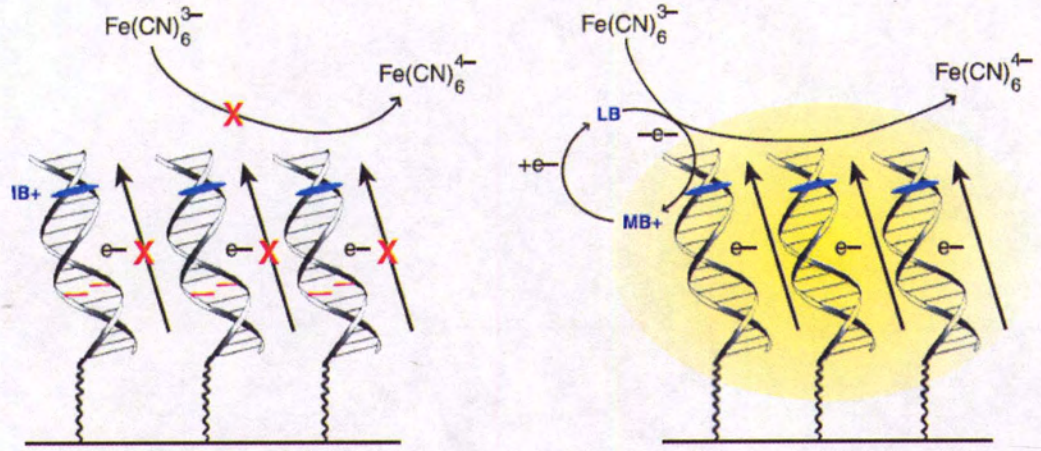

Figure 1-5 Electrochemical assay for mismatches through DNA-mediated charge transport. [Adapted by permission from Ref. 6]

The use of enzyme labels also promises sensitive electrochemical detection of DNA hybridization. Heller's group demonstrated that a direct low-potential amperometric detection of DNA hybridization event can be achieved by using horseradish-peroxidase labeled targets.[23] In this case, the hybridization of enzyme-labeled target DNA with the probe DNA results in the "wiring" of the enzyme to the transducer (electrode) and then generates a continuous hydrogen-peroxide reduction current. Similar enzyme-labeled DNA sensors have been proposed by other researchers.[24]

1.4 Metal Ion-DNA Interactions

Nucleic acids are negatively charged polymers that interact reversibly with a broad range of metal ions and their complexes, and "condense (adsorb)" a significant

number of them from solution to achieve stable conformations.[1b] Metal ion-DNA interactions are also important for DNA replication and transcription in *vivo*, and can be exploited for the development of DNA-targeted drugs and biosensors.[25] Alkali and alkaline earth metal cations (mainly Na^+, K^+, Mg^{2+}, and Ca^{2+}) are present in human body in millimolar concentrations and bind to DNA electrostatically, usually mediated by water. They become toxic if the concentrations surpass the natural levels. Their depletion may also cause diseases. For example, deficiency of iron, magnesium or calcium causes may anaemia, cardiovascular diseases or osteoporosis, respectively.[25a]

The interactions between double helical DNA and ions, specifically mono- and divalent metal cations, have been investigated extensively during the past 30 years. These positively charged metal ions interact directly or indirectly with sites characterized by high electron density or negatively charged residues of DNA.[25]

Transition metal complexes interact with more than two different sites and their interactions with DNA are more complicated. They can loose their water molecules easily and give inner sphere coordinated complexes.[25a] There are two types of interaction modes in general: electrostatic attraction and intercalation into the hydrophobic regions of the DNA. The mode is dependent on the molecular structure of the complex and the ionic strength of the environment and can be managed by choosing appropriate metal chelating ligands. For instance, tris-chelated ruthenium, cobalt or iron complexes with 1,10-phenanthroline (phen) interact with duplex DNA via intercalation, while analogous 2,2'-bipyridine (bipy) chelates of ruthenium or osmium bind to DNA electrostatically.[3]

Conventional approaches to study metal ion-DNA interactions include molecular dynamic simulation, solution NMR, and X-ray crystallography.[25] Spectroscopic and X-

ray diffraction data show that there are four preferential sites for metal binding: the N7 atom of purine, N3 of pyrimidine residues, exocyclic oxygen and the phosphate oxygen atoms.[25a] MD simulations, solution NMR, and crystallographic results exclusively show that the monovalent cations Na^+, K^+, Rb^+, Cs^+ and NH_4^+ prefer direct binding (inner sphere) to AT rich region of the DNA minor groove.[26] Magnesium (Mg^{2+}) is the major intracellular divalent ion from the group of alkaline earth metals and is present in all DNA and RNA activation processes. Using Fourier transform infrared and Raman as well as NMR spectroscopy, it was found that magnesium ions play a significant role in the stabilization of secondary and tertiary structure of the DNA.[25] Transition metals usually bind directly to the bases and indirectly to the phosphate groups. For example, FT-IR spectra shows that Mn^{2+} cations form zwitterionic type complex with 5'-guanosine monophosphate by replacing the sodium cations of the phosphate group.[25a, 27]

1.5 Previous Work and Objectives of This Thesis

1.5.1 Voltammetric Procedure for Examining DNA-Modified Surfaces

In a recent publication from our laboraotry,[28] a simple electrochemical procedure was proposed to study DNA-modified surfaces, including DNA probe quantitation, cation binding thermodynamics, and electron-transfer kinetics. It is based on the voltammetric behavior of multiply charged transition metal cations bound electrostatically to DNA strands. The key feature of our approach is the easy distinction of the surface peaks from the signals of diffused species by using micromolar concentrations (μM) of the redox molecules.[28] In comparison with other electrochemical methods,[11c-d, 29, 30] the attractive aspects of this technique are its experimental simplicity and the ease of interpretation of the results.

1.5.1.1 Cyclic Voltammetry

Cyclic voltammetry (CV) is one of the most popular techniques to characterize the redox behavior of compounds and to elucidate the kinetics of electrode reactions.[31] Typically, an electrochemical cell for CV measurements contains three different electrodes: working, reference, and counter electrode. The current flows between the working and counter electrode (ideally the electronic circuitry ensures that no current will flow through the reference). The potential is controlled relative to the reference electrode. In CV, the current in the cell is measured as a function of potential. During the measurement, the potential of working electrode is linearly cycled from a starting to a final potential, and then back to the starting potential. This process, in turn cycles the redox reaction. A plot of potential versus current is then produced, which is the so-called cyclic voltammogram.[31] In this thesis, an one-compartment and three-electrode Teflon cell was used for the measurements (Figure 1-7). Bare or DNA modified gold slides were used as working electrodes and pressed against an O-ring seal at the cell bottom (with an exposed area of 0.68 cm^2). An Ag | AgCl | 3M NaCl electrode was used as reference electrode, and the counter electrode was a Pt wire.

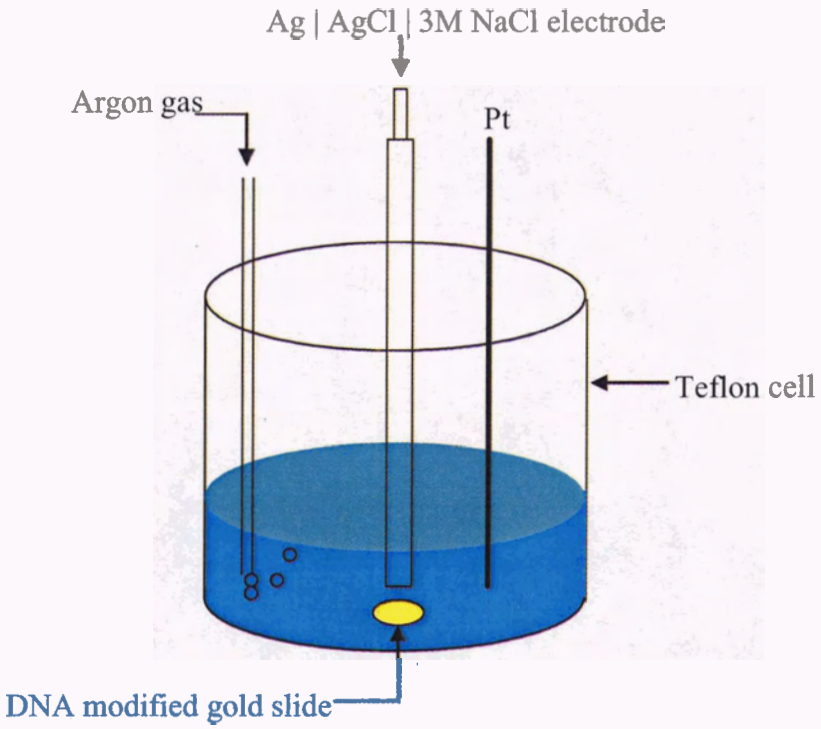

Figure 1-6 Schematic representation of the electrochemical cell for cyclic voltammetric measurements of DNA modified gold electrodes.

1.5.1.2 Quantitation of DNA Probes

Upon prolonged incubation (e.g. 2 hrs) in a solution containing multiply charged metal complexes, such as $[Ru(NH_3)_6]^{3+}$, at low ionic strength, an ion-exchange equilibrium between these transition metal cations and the native charge compensation ions M^+ (presumably Na^+ and $Tris^+$) associated with the anionic DNA backbone is established.[21, 28] The reaction assumes that the penetration of the DNA monolayers by $[Ru(NH_3)_6]^{3+}$ results in ejection of M^+ on a 1:1 (charge) basis, which is certainly true when the concentration of metal cations is high and the incubation time is adequate. The cyclic voltammetry that results from partitioning $[Ru(NH_3)_6]^{3+}$ into DNA monolayers is shown in figure 1-7.

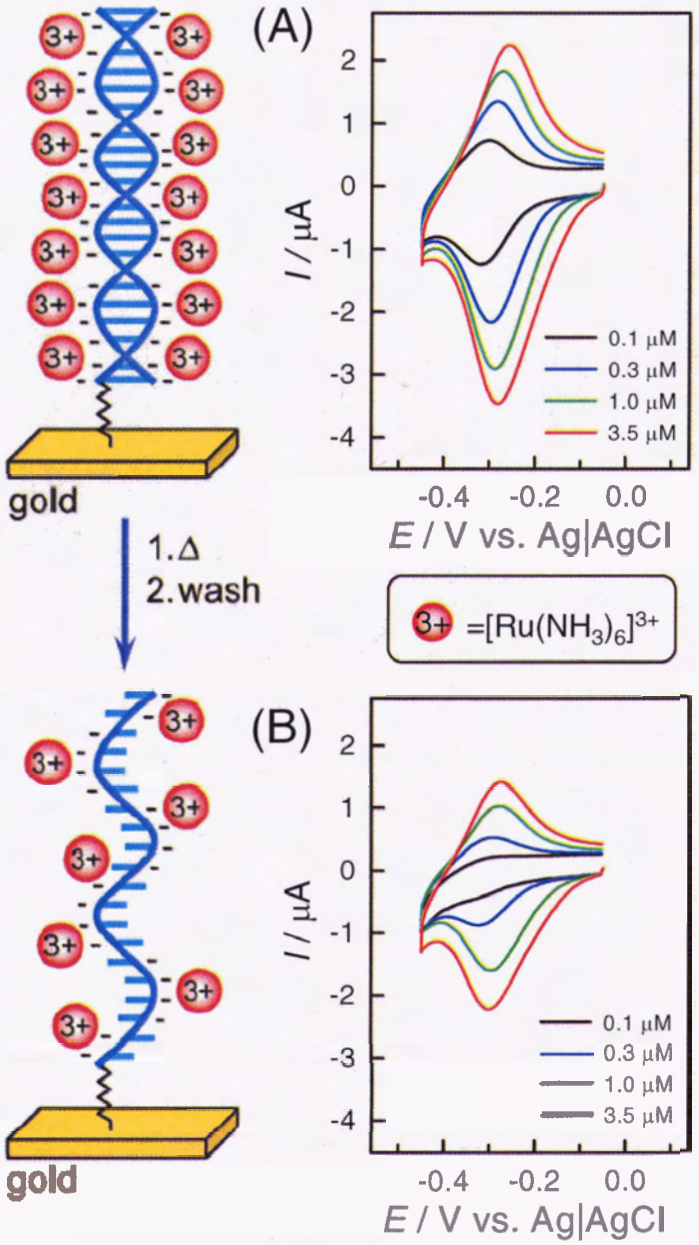

Figure 1-7 **Pictorial representation and voltammetric response of multiply-charged transition metal complexes bound electrostatically to DNA-modified surfaces: cyclic voltammograms of gold electrodes modified with dsDNA (A) and ssDNA (B) in 10 mM Tris buffer (pH7.4) in the presence of $[Ru(NH_3)_6]^{3+}$ at different concentrations as listed. The scan rate was 50 mV/s. [Adapted by permission from ref. 28]**

Then the surface concentration of $[Ru(NH_3)_6]^{3+}$, Γ_{Ru} (mol/cm^2) can be easily determined from eq. (1):

$$\Gamma_{Ru} = \frac{Q}{nFA} \tag{1}$$

where Q is the charge that can be obtained from the integration of the reduction peak of surface-bound $[Ru(NH_3)_6]^{3+}$, n is the number of electrons in the reaction, and A is the electrode area. The peak area for integration normally is obtained by subtracting the background, which is obtain in the solution free of redox cations, from the voltammetric signal of the $[Ru(NH_3)_6]^{3+}$ (as shown in figure 1-8).

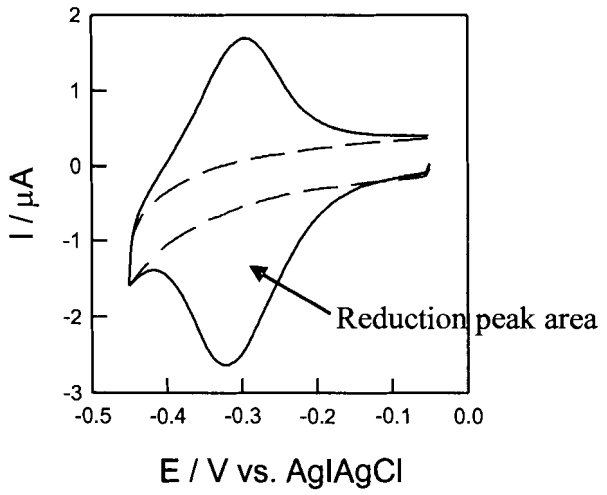

Figure 1-8 Cyclic voltammograms of dsDNA/Au in 10mM Tris buffer in the absence(dashed line) and presence(solid line) of 3.5μM redox cation $[Ru(NH_3)_6]^{3+}$. The scan rate is 50 mV/s.

Furthermore, based on the saturation quantity of $[Ru(NH_3)_6]^{3+}$, the measure value can be directly converted to the surface density of DNA probes based on eq. (2):

$$\Gamma_{DNA} = \Gamma_{Ru}(\frac{z}{m})N_A \qquad (2)$$

where m is the number of nucleotides in the DNA, z is the charge of the redox cation, and N_A is Avogadro's number. The surface densities, Γ_{DNA}, for the electrodes modified with dsDNA and ssDNA that evaluated from the voltammetric concentration of $[Ru(NH_3)_6]^{3+}$ are $4.6\pm0.6\times10^{12}$ molecule/cm^2 and $5.3\pm0.4\times10^{12}$ molecule/cm^2 respectively. These values are close to the theoretical estimation (5.2×10^{12} molecule/cm^2)[11c], which is calculated by assuming that the DNA monolayers are compact and the double helices "stand" on the surface with a small tilt angle relative to the normal.

1.5.1.3 Cationic Binding Activity Study Based on Langmuir Model

Langmuir derived a simple model involving a thermodynamic equilibrium to predict the fraction of solid surface covered by an adsorbate as a function of its gas pressure in 1916.[32] This was later extended to liquid systems, where the equilibrium involved concentrations in solution. This classical model assumes that every binding site is equivalent; the ability of a molecule to bind is independent of occupation of nearby sites; and the activity of the adsorbate is directly proportional to its concentration.[28] The derivation of the Langmuir isotherm for cation-DNA binding equilibrium is[21b, 28]

$$\frac{C}{Q} = \frac{C}{Q_{sat}} + \frac{1}{KQ_{sat}} \qquad (3)$$

where C is the concentration of the redox cation $[Ru(NH_3)_6]^{3+}$ solution, Q is the accumulated charge at the electrode surface, Q_{sat} is the saturated charge, and K is the equilibrium binding constant.

The voltammetric response as a function of the solution concentration of $[Ru(NH_3)_6]^{3+}$ has been analyzed by fitting to the Langmuir isotherm given in eq. (3).[14b, 19] The linearity of the plot of C/Q vs. C indicated that the binding isotherm can be described by eq. (3), and the values of the interaction equilibrium constants of $[Ru(NH_3)_6]^{3+}$ with both dsDNA and ssDNA modified surfaces were thus obtained, which are $2.0\pm0.5\times10^6$ M^{-1} and $1.5\pm0.5\times10^6$ M^{-1} for respectively.[28]

1.5.2 Design of Deoxyribosenors for Specific Detection of Molecular Analytes

The dependence of the DNA conductivity on its conformational state can be used to design biosensors.[33] During the past few years, Dr. Sen's group has successfully incorporated aptamers (nucleic acid receptors) into DNA structures such that ligand binding would switch the conformation of the DNA assembly. These deoxyribosenors only permit electrical conduction through the entire DNA structure in the presence of a bound analyte.[33]

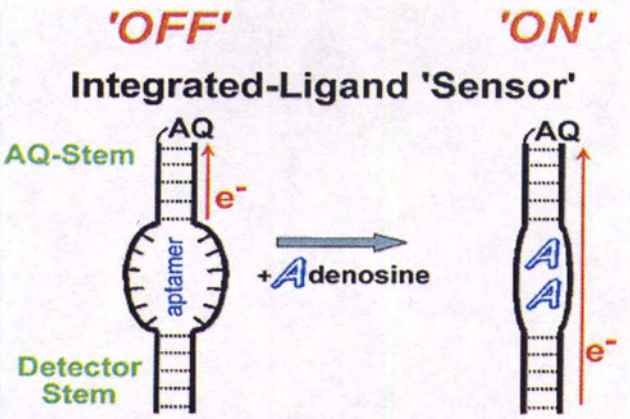

Figure 1-9 Design of the "integrated-ligand" deoxyribosensor. In the absence of the ligand / analyte (adenosine) the sensor adopts an open, unstructured conformation, which only allows charge transfer (indicated by red arrows) from the AQ stem. [Adapted by permission from ref. 33]

As shown in Figure 1-9, one strand of the DNA double helix was labeled by the light-activated photo-oxidant, anthraquinone (AQ), for initiation of charge transport. In the absence of adenosine, the aptamer region separates the Watson-Crick base-paired AQ and a "detector" double helical stem, which interrupts the electron transfer from the detector stem. The DNA aptamer sequence used here has been *in vitro* selected for a trial analyte, adenosine, which binds poorly, if at all, to double-stranded DNA.[34] NMR studies have shown that the binding of one aptamer molecule to two adenosine molecules compacted the aptamer's loose structure to a tightly hydrogen-bonded and base-stacked helical structure,[35] which allows electron transfer between the AQ and the detector stems.[33]

1.5.3 Objectives of This Thesis

To augment our fundamental understanding of metal ion-DNA interactions, we initiated electrochemical studies of metal ion-DNA interactions on surfaces using the previously reported simple protocol developed in our laboratory previously.[33] Past investigations have been focused on the thermodynamics of ionic binding,[33] partially due

to the fact that the kinetics are difficult to monitor in solution under homogenous conditions. However, on a gold surface, the high density and ordered orientation of the immobilized DNA strands are expected to slow down the ion transport in and out of the DNA monolayer, thereby permitting kinetic investigations. The examination of the relative binding abilities of biological relevant metal cations (e.g., magnesium, calcium, and potassium ions) to DNA, and the construction of deoxyribosensors for direct electrochemical detection of molecular analytes were also of considerable interest to us.

Chapters 2, 3, and 4, respectively, describe the results of our voltammetric experiments a) to monitor the kinetics of the $[Ru(NH_3)_6]^{3+}$ interactions with thiolate-DNA monolayers on gold, b) to determine the selectivity of metal cations (Mg^{2+}, Ca^{2+}, and K^{+}) binding to DNA, and c) to develop deoxyribosensors incorporating ATP/adenosine aptamer in DNA monolayers on gold electrode for specific detection of molecular analytes.

1.6 Reference

1. Campbell, M. K. *Biochemistry,* 3rd Edition, Harcourt Brace Publishers, Philadelphia, **1999**, (a) pp 20-22. (b) pp 251-258.
2. Watson, J. D.; Crick, F. H. C. *Nature* **1953**, *171*, 737-738.
3. Fojta, M. *Electroanalysis* **2002**, *14*, 1449-1463.
4. For example of recent reviews of DNA chips see: (a) Pirrung, M. C. *Angew. Chem. Int. Ed.* **2002**, *41*, 1276-1289. (b) Blohm, D. H.; Guiseppi-Elie, A. *Curr. Opin. Biotechnol.* **2001**, *12*, 41-47. (c) Wang, J. *Nucleic Acid Res.* **2000**, *28*, 3011-3016. (d) Freeman, W. M.; Robertson, D. J.; Vrana, K. E. *BioTechniques* **2000**, *29*, 1042-1046. (e) Niemeyer, C. M.; Blohm, D. H. *Angew. Chem. Int. Ed.* **1999**, *38*, 2865-2869.
5. www.affymetrix.com, accessed on November 13, 2004.
6. Drummond, T. G.; Hill, M. G.; Barton, J. K. *Nat. Biotechnol.* **2003**, *21*, 1192-1199.

7. Steel, A. B.; Levicky, R. L.; Herne, T. M.; Tarlov, M. J. *Biophy. J.* **2000**, *79*, 975-981.

8. (a) Pease, A. C.; Solas, D.; Sullivan, E. J.; Cronin, M. T.; Holmes, C. P.; Fodor, S. *Proc. Natl. Acad. Sci. USA.* **1994**, *91*, 5022-5026. (b) Southerm, E. M.; Case-Green, S. C.; Elder, J. K.; Johnson, M.; Mir, K. U.; Wang, L.; Williams, J. C. *Nucleic Acids Res.* **1994**, *22*, 1368-1373.

9. (a) O'Donnell, M. J.; Tang, K.; Koster, H.; Smith, C. L.; Cantor, C. R. *Anal. Chem.* **1997**, *69*, 2438-2443. (b) Gingeras, T. R.; Kwoh, D. Y.; Davis, G. R. *Nucleic Acids Res.* **1987**, *15*, 5373-5390.

10. Wang, J. *Anal. Chim. Acta,* **2002**, *469*, 63-71.

11. For examples of studies of thiolate DNA-monolayers on gold, see, (a) Herne, T. M.; Tarlov, M. J. *J. Am. Chem. Soc.* **1997**, *119*, 8916-8920. (b) Kelley, S. O.; Jackson, N. M.; Hill, M. G.; Barton, J. K. *Angew. Chem. Int. Ed.* **1999**, *38*, 941-945. (c) Yu, C. J.; Wan, Y. J.; Yowanto, H.; Li, J.; Tao, C. L.; James, M. D.; Tan, C. L.; Blackburn, G. F.; Meade, T. J. *J. Am. Chem. Soc.* **2001**, *123*, 11155-11161. (d) Kertesz, V.; Whittemore, N. A.; Chambers, J. Q.; McKinney, M. S.; Baker, D. C. *J. Electroanal. Chem.* **2000**, *493*, 28-36. (e) Hartwich, G.; Caruana, D. J.; de Lumley-Woodyear, T.; Wu, Y. B.; Campbell, C. N.; Heller, A. *J. Am. Chem. Soc.* **1999**, *121*, 10803-10812.

12. (a) Finklea, H. O. *Encyclopedia of Analytical Chemistry: Electrochemical Method-Self-Assembly Monolayers,* John Wiley & Sons: New York, **2000**. (b) Ulman, A. *An Introduction to Ultrathin Organic Films: from Langmuir-Blodgett to Self-Assembly*, Academic press: San Diego, **1991**; pp 279-297.

13. (a) Levicky, R.; Herne, T. M.; Tarlov, M. J.; Satija, S. K. *J. Am. Chem. Soc.* **1998**, *120*, 9787-9792. (b) Aqua, T.; Naaman, R.; Daube, S. S. *Langmuir* **2003**, *19*, 10573-10580.

14. For example see, (a) Peterlinz, K. A.; Georgiadis, R. M.; Herne, T. M.; Tarlov, M. J. *J. Am. Chem. Soc.* **1997**, *119*, 3401-3402. (b) Csaki, A.; Moller, R.; Straube, W.; Kohler, J. M.; Fritzsche, W. *Nucleic Acids Res.* **2001**, *29*, e81. (c) Kelly, S. O.; Barton, J. K. *Bioconjugate Chem.* **1997**, *8*, 31-37. (d) Brewer, S. H.; Anthireya, S. J.; Lappi, S. E.; Drapcho, D. L.; Franzen, S. *Langmuir*, **2002**, *18*, 4460-4464.

15. Palecek, E. *Nature* **1960**, *188*, 656-657.

16. For recent reviews of DNA-based electrochemical sensors, see (a) de-los-Santos-Alvarez, P.; Lobo-Castanon, M. J.; Miranda, A. J.; Tunon-Blanco, P. *Anal. Bioanal. Chem.* **2004**, *378*, 104-118. (b) Vercoutere, W.; Akeson, M. *Curr. Opin. Chem. Biol.* **2002**, *6*, 816-822. (c) Wang, J. *Chem. Eur. J.* **1999**, *5*, 1681-1685.

17. Palecek, E. *Anal. Biochem.* **1988**, *170*, 421-431.

18. (a) Jelen, F.; Yosypchuk, B.; Kourilova, A.; Novotny, L.; Palecek, E. *Anal. Chem.* **2002**, *74*, 4788-4793. (b) Wang, J.; Kawde, A. B. *Analyst*, **2002**, *127*, 383-386.

19. Yang, I. V.; Thorp, H. H. *Anal. Chem.* **2001**, 73, 5316-5322.

20. (a) Millan, K. M.; Mikkelsen, S. R. *Anal. Chem.* **1993**, *65*, 2317-2323. (b) Millan, K. M.; Saraullo, A.; Mikkelsen, S. R. *Anal. Chem.* **1994**, *66*, 2943-2948.

21. (a) Steel, A. B.; Herne, T. M.; Tarlov, M. J. *Anal. Chem.* **1998**, *70*, 4670-4677. (b) Steel, A. B.; Herne, T. M.; Tarlov, M. J. *Bioconjugate Chem.* **1999**, *10*, 419-423.

22. Boon, E. M.; Ceres, D. M.; Drummond, T. G.; Hill, M. G.; Barton, J. K. *Nat. Biotechnol.* **2000**, *18*, 1096-1100.

23. Campbell, C. N.; Gal, D.; Cristler, N.; Banditrat, C.; Heller, A. *Anal. Chem.* **2002**, *74*, 158-162.

24. (a) Azek, F.; Grossiord, C.; Joannes, M.; Limoges, B.; Brossier, P. *Anal. Biochem.* **2000**, *284*, 107- 113. (b) Patolsky, F.; Katz, E.; Willner, I. *Angew. Chem. Int. Ed.* **2002**, *41*, 3398-3402.

25. (a) Anastassopoulou, J. *J. Mol. Struc.* **2003**, *651*, 19-26. (b) Egli, M. *Chem. Biol.* **2002**, *9*, 277-286.

26. (a) Tereshko, V.; Wilds, C. J.; Minasov, G.; Prakash, T. P.; Maier, M. A.; Howard, A.; Wawrzak, Z.; Manoharan, M.; Egli, M. *Nucleic Acids Res.* **2001**, *29*, 1208-1215. (b) Stelwagen, N. C.; Magnusdottir, S.; Gelfi, C.; Righeti, P. G. *J. Mol. Biol.* **2001**, *305*, 1025-1033.

27. Anastassopoulou, J.; Barbarossou, K.; Korbaki, V.; Theophanides, T.; Legrand, P.; Huvenne, J-P.; Sombert, B. *Spectroscopy of Biological Molecules*, vol. 7, Kluwer Academic Publishers, Dordrecht, The Netheralnds, 1997, pp 233.

28. Yu, H. Z.; Luo, C. Y.; Sankar, C. G.; Sen, D. *Anal. Chem.* **2003**, *75*, 3902-3907.

29. Whittemore, N. A.; Mullenix, A. N.; Inamati, G. B.; Manoharan, M.; Cook, P. D.; Tuinman, A. A.; Baker, D. C.; Chambers, J. Q. *Bioconjugate Chem.* **1999**, *10*, 261-270.

30. (a) Patolsky, F.; Weizmann, Y.; Willner, I. *J. Am. Chem. Soc.* **2002**, *124*, 770-772. (b) Patolsky, F.; Katz, E.; Willner, I. *Angew. Chem. Int. Ed.* **2002**, *41*, 3398-3402. (c) Gore, M. R.; Szalai, V. A.; Ropp, P. A.; Yang, I. V.; Silverman, J. S.; Thorp, H. H. *Anal. Chem.* **2003**, *75*, 6586-6592. (d) Kim, E.; Kim, K.; Yang, H.; Kim, Y. T.; Kwak, J. *Anal. Chem.* **2003**, *75*, 5665-5672.

31. (a) Van Benschoten, J. J.; Lewis, J. Y.; Heineman, W. R.; Roston, D. A.; Kissinger, P. T. *J. Chem. Ed.* **1983**, *60(9)*, 772-776. (b) Kissinger, P. T.; Heineman, W. R. J. Chem.Ed. 1983, *60(9)*, 702-706. (c) Harris, D. C. *Quantitative Chemical Analysis*, Sixth Edition, Michelle Russel Julet, New York, **2002**, pp394-396.

32. Langmuir, I. *J. Am. Chem. Soc.* **1916**, *38*, 2221-95.

33. Fahlman, R. P.; Sen, D. *J. Am. Chem. Soc.* **2002**, *124*, 4610-4616.

34. Huizenga, D. E.; Szostak, J. W. *Biochemistry* **1995**, *34*, 656-665.

35. Lin, C. H.; Patel, D. J. *Chem. Biol.* **1997**, *4*, 817-832.

CHAPTER 2
KINETICS OF ION-EXCHANGE BINDING OF REDOX METAL CATIONS TO THIOLATE-DNA MONOLAYERS ON GOLD

In this chapter, the kinetics of the ion-exchange binding of redox metal cations to thiolate-DNA monolayers on gold was investigated using a simple electrochemical protocol. Starting from the introduction to related literature work, this chapter describes the time-dependent voltammetric behaviour of redox cations bound to DNA monolayers and the subsequent theoretical evaluation of the kinetic parameters. The kinetic data augment our fundamental understanding of metal ion-DNA interactions, and are critical for the evaluation of the accuracy and reliability of experimental DNA detection protocols.

2.1 Introduction

The thermodynamics (adsorption isotherm and equilibrium constants) of cation-DNA interactions have been studied in great details in the past as discussed in Chapter 1. In contrast, very little is known about the binding kinetics of metal cations to DNA either in solution or on surfaces,[1] though electrochemical methods have long been used to study the kinetics of the adsorption of conventional molecules and molecular recognition on surfaces.[2-5] Horrocks et al. noted that cyclic voltammetry could detect binding kinetics, but did not provide further investigation or interpretation.[6] Pang et al. reported their brief kinetics study of the interactions between benzyl viologen (BV) and calf-thymus DNA adsorbed on gold surfaces.[1] In our study, a multiply charged transition metal cation,

$[Ru(NH_3)_6]^{3+}$, was chosen as model system, partially because of its ideal electrochemical response.[7, 8] The analogous transition metal complex $[Co(NH_3)_6]^{3+}$ has been widely used as a "biochemically inert" substitute for the alkaline earth metals (e.g., Mg^{2+}, which interacts in the form of $[Mg(H_2O)_6]^{2+}$ with DNA/RNA) because of similar size and octahedral geometry (although different charge) of the two molecules.[9,10]

2.2 Experimental Section

Materials. The synthetic DNA oligonucleotide 5'TTTAGCTGACGTCAGATC-GA3' and the disulfide derivative of its complementary strand, DMT-O-C6-S-S-C6-O-5'TCGATCTGACGTCAGCTAAA3', were purchased from Core DNA Services Inc. (Calgary, AB). The 5'-thiol modifier was from Glen Research (Sterling, VA). The DMT (dimethoxytrityl) group protects the disulfide and serves as an appropriate hydrophobic group for HPLC purification.

Glass slides coated with 10 nm titanium (to improve adhesion) and 100 nm gold were obtained from Evaporated Metal Film (EMF) Inc. (Ithaca, NY). 6-Mercapto-1-hexanol (MCH) and hexaammine ruthenium (III) chloride (98%) were obtained from Sigma-Aldrich (Milwaukee, WI) and used as received. Deionized water (>18.3 MΩ·cm) was from a Barnstead EasyPure UV/UF compact water system (Dubuque, IA). Different buffers were employed for specific experimental tasks. For DNA hybridization and immobilization, 10 mM Tris buffer / 0.1 M $MgCl_2$ / 1 M NaCl at pH 7.4 (buffer A) was used. Electrodes were rinsed successively with 10 mM Tris buffer / 50 mM NaCl, pH 7.4 (buffer B) and 10 mM Tris buffer / 10 mM NaCl, pH 7.4 (buffer C). Electrochemical characterizations were performed in 10 mM Tris buffer (at pH 7.4) containing different concentrations of $Ru(NH_3)_6Cl_3$.

DNA Purification. The disulfide-derivatized oligomer was deprotected with saturated $NH_3 \cdot H_2O$ at 55 °C for 12 h and then purified by reversed-phase HPLC on a C18 Vydac Column (218TP54). The sample was then treated with 100 mM DTT (dithiothreitol) at pH 8.5 for 30 min and passed through a Pharmacia Nap-5 Column (G-25 Sephadex) to yield pure thiol-tethered ssDNA, HS-C6-O-5'TCGATCTGACGTC-AGCTAAA3'.

Surface Preparation. The gold-coated slides (2×2 cm^2) were cleaned by immersion in a "piranha" solution" (a mixture of 70% concentrated sulfuric acid and 30% hydrogen peroxide) for 5 min at about 90 °C. *WARNING: piranha solution reacts violently with organic solvents, and should be handled with extreme care.* They were rinsed thoroughly with deionized water and dried under N_2. Gold electrodes modified with single-stranded DNA (ssDNA/Au) were prepared by spreading 100 μL of 10 μM solution of the thiol-terminated ssDNA in buffer A over the cleaned gold surface for 1 min to 24 h (in order to control the surface density of the DNA strands) at ambient conditions. After modification, the sample was rinsed with buffer B, buffer C, and 10 mM Tris buffer, immersed in a 1.0 mM MCH solution for 1 h, rinsed again with 10 mM Tris buffer and dried under N_2 before characterization. To prepare gold electrodes modified with double-stranded DNA (dsDNA/Au), we first hybridized the 10 μM solution of the thiol-terminated ssDNA in deoxygenated buffer A with its complementary strand by heating to 90 °C followed by slow cooling to room temperature, and then used the procedure described above for the preparation of ssDNA/Au.

Instrumentation. Cyclic voltammetry was performed with a μAutolab II potentiostat / galvanostat (EcoChemie B.V., Utrecht, The Netherlands). A one-

compartment and three-electrode Teflon cell was used for the measurements. Gold slides modified with double-stranded (dsDNA/Au) or single-stranded (ssDNA/Au) oligonucleotides were used as working electrodes and pressed against an O-ring seal at the cell bottom (with an exposed area of 0.68 cm^2). An Ag | AgCl | 3M NaCl electrode was used as reference electrode, and the counter electrode was a Pt wire.

2.3 Results and Discussions

Upon prolonged incubation (e.g 2 hrs) in a solution containing multiply charged metal complexes, such as $[Ru(NH_3)_6]^{3+}$, at low ionic strength, an ion-exchange equilibrium between these transition metal cations and the native charge compensation ions M^+ (presumably Na^+ and $Tris^+$) associated with the anionic DNA backbone is established.[7, 8] As is introduced in chapter one, values of the surface concentration of $[Ru(NH_3)_6]^{3+}$ (Γ_{Ru}) and the surface density of DNA (Γ_{DNA}) can be calculated based on the integrated charge of redox peaks. At low concentrations of metal cations (< 5.0 μM), a clear time-dependence of the voltammetric behavior of the immobilized redox cations has been observed (Figure 2-1).

2.3.1 Evaluation of Apparent First-Order Rate Constants

Figure 2-1 shows the representative responses obtained when gold electrodes modified with ssDNA (A) and dsDNA (B) were used to record voltammograms in 0.5 and 2.5 μM $[Ru(NH_3)_6]^{3+}$ solutions, respectively. During the incubation period, the solution was stirred by bubbling argon gas, in order to minimize the possible depletion of

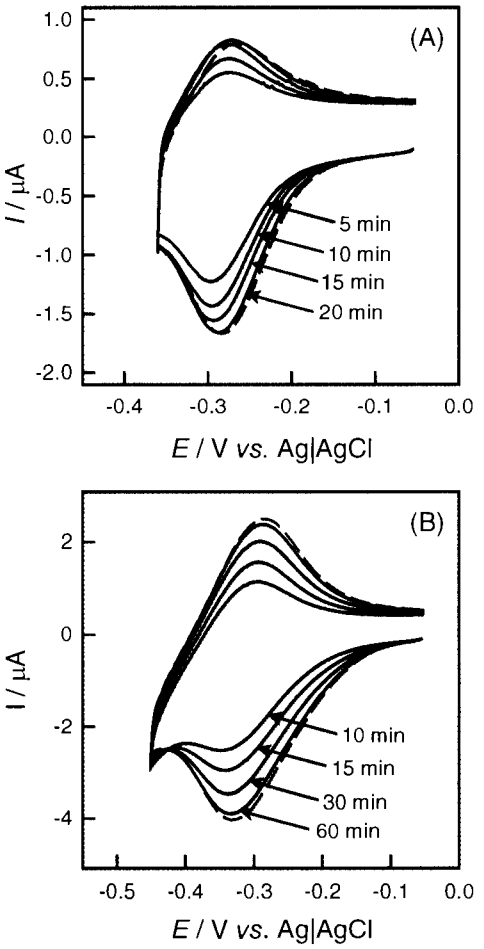

Figure 2-1 Cyclic voltammograms of 0.5 μM $[Ru(NH_3)_6]^{3+}$ on ssDNA/Au (A) and of 2.5 μM $[Ru(NH_3)_6]^{3+}$ on dsDNA/Au (B). The dashed lines show the steady state CVs (i.e., after prolonged incubation (e.g 2 hrs) in the $[Ru(NH_3)_6]^{3+}$ containing electrolyte). The electrolyte is 10 mM Tris buffer at pH 7.4, and the scan rate is 50 mV/s.

the reactant at the electrode surface. We believe that the slow adsorption process (tens to hundreds of minutes to reach equilibrium) is not significantly influenced by the mass-transport of $[Ru(NH_3)_6]^{3+}$ to the electrode surface. It is clear that both the cathodic and anodic currents increase significantly with increasing incubation time before equilibrium is reached. The outmost curves are the equilibrium CVs that were recorded after

prolonged incubation. In all cases, the voltammetric responses are due to the surface-bound $[Ru(NH_3)_6]^{3+}$; contributions from the solution-diffused species are negligible.[8] The development of the voltammetric signal as a function of time shown in Figure 2-1 contrasts with that recorded by Steel et al.[7b] for ssDNA-modified gold electrodes. The extra set of waves in their CVs is due to diffused species resulting from the much higher concentration of redox cations, also $[Ru(NH_3)_6]^{3+}$ (50 μM) used in their experiments. For the same reason, the kinetic development of the voltammetric signal was not noticeable; rather, the repeated scans were essentially overlapping.[7b] The time-dependent behavior observed in Figure 2-1 is similar to the voltammetric response reported for the binding of $[Ru(NH_3)_6]^{3+}$ to a graphite electrode modified with polyvinyl sulfate,[11] a anionic polyelectrolyte.

The well-behaved voltammetric response and intriguing difference between the time scales for ssDNA/Au and dsDNA/Au deserve further theoretical consideration. Since the surface quantity of $[Ru(NH_3)_6]^{3+}$ can be readily determined by integration of the cathodic peak, we can quantitatively analyze the kinetics of redox cation-DNA interactions on surfaces. The ion-exchange binding can be expressed in the form of eq. (1), (2), (3), where the replacement of the native charge compensation ions M^+ by the multiply charged metal cations in solution ($[Ru(NH_3)_6]^{3+}$) consequently, is explicitly included.

$$DNA \cdot 3M^+ + Ru^{3+}_{soln} \underset{k_{-1}}{\overset{k_{+1}}{\rightleftharpoons}} DNA \cdot 2M^+Ru^{3+} + M^+_{soln} \quad (1)$$

$$DNA \cdot 2M^+Ru^{3+} \underset{k_{-2}}{\overset{k_{+2}}{\rightleftharpoons}} DNA \cdot M^+Ru^{3+} + M^+_{soln} \quad (2)$$

$$DNA \cdot M^+Ru^{3+} \underset{k_{-3}}{\overset{k_{+3}}{\rightleftharpoons}} DNA \cdot Ru^{3+} + M^+_{soln} \quad (3)$$

where $DNA \cdot 3M^+$ is three monocation exchangeable complex, $DNA \cdot 2M^+Ru^{3+}$ is two monocation exchangeable complex, $DNA \cdot M^+Ru^{3+}$ is one monocation exchangeable complex, $DNA \cdot Ru^{3+}$ is surface-bound redox cation $[Ru(NH_3)_6]^{3+}$, Ru^{3+}_{soln} is $[Ru(NH_3)_6]^{3+}$ in solution, k_{+1}, k_{+2}, k_{+3} and k_{-1}, k_{-2}, k_{-3} are the binding and dissociation rate constants. In the following derivation, square brackets to denote surface concentrations as well as solution concentrations are used for clarity.

The rate laws for these three reactions are:

$$\frac{d[DNA \cdot 2M^+Ru^{3+}]}{dt} = k_{+1}[DNA \cdot 3M^+][Ru^{3+}]_{soln} - k_{-1}[DNA \cdot 2M^+Ru^{3+}] \cdot [M^+]_{soln} - k_{+2}[DNA \cdot 2M^+Ru^{3+}] + k_{-2}[DNA \cdot M^+Ru^{3+}] \cdot [M^+]_{soln} \quad (1)'$$

$$\frac{d[DNA \cdot M^+ \cdot Ru^{3+}]}{dt} = k_{+2}[DNA \cdot 2M^+Ru^{3+}] - k_{-2}[DNA \cdot M^+Ru^{3+}] \cdot [M^+]_{soln} - k_{+3}[DNA \cdot M^+Ru^{3+}] + k_{-3}[DNA \cdot Ru^{3+}] \cdot [M^+]_{soln} \quad (2)'$$

$$\frac{d[DNA \cdot Ru^{3+}]}{dt} = k_{+3}[DNA \cdot M^+Ru^{3+}] - k_{-3}[DNA \cdot Ru^{3+}] \cdot [M^+]_{soln} \quad (3)'$$

In these consequent reactions, $DNA \cdot 2M^+Ru^{3+}$ and $DNA \cdot M^+Ru^{3+}$ are intermediates, so both eq. (1)' and (2)' should be close to zero based on the steady state assumption. From eq. (1)' ≈0, one can get:

$$[DNA \cdot 2M^+Ru^{3+}] = \frac{k_{+1}[DNA \cdot 3M^+][Ru^{3+}]_{soln} + k_{-2}[DNA \cdot M^+Ru^{3+}][M^+]_{soln}}{k_{-1}[M^+]_{soln} + k_{+2}} \quad (4)$$

From eq. (2)' ≈0, one can get:

$$[DNA \cdot M^+Ru^{3+}] = \frac{k_{+2}[DNA \cdot 2M^+Ru^{3+}] + k_{-3}[DNA \cdot Ru^{3+}][M^+]_{soln}}{k_{-2}[M^+]_{soln} + k_{+3}} \quad (5)$$

Substituting eq. (4) into eq. (5) leads to:

$$[DNA \cdot M^+Ru^{3+}] = \frac{k_{+1}k_{+2}[DNA \cdot 3M^+][Ru^{3+}]_{soln} + k_{-1}k_{-3}[DNA \cdot Ru^{3+}][M^+]^2_{soln} + k_{+2}k_{-3}[DNA \cdot Ru^{3+}][M^+]_{soln}}{k_{-1}k_{-2}[M^+]^2_{soln} + k_{-1}k_{+3}[M]_{soln} + k_{+2}k_{+3}} \quad (6)$$

Then substitute into eq. 3' results in:

$$\frac{d[DNA \cdot Ru^{3+}]}{dt} = \left(\frac{k_{+1}k_{+2}k_{+3}}{k_{-1}k_{-2}[M^+]^2_{soln} + k_{-1}k_{+3}[M^+]_{soln} + k_{+2}k_{+3}}\right) \cdot [DNA \cdot 3M^+] \cdot [Ru^{3+}]_{soln} - \left(\frac{k_{-1}k_{-2}k_{-3}[M^+]^3_{soln}}{k_{-1}k_{-2}[M^+]^2_{soln} + k_{-1}k_{+3}[M^+]_{soln} + k_{+2}k_{+3}}\right) \cdot [DNA \cdot Ru^{3+}] \quad (7)$$

The concentration of $[M^+]_{soln}$ remains constant during the reaction as the concentration of monocation (determined by the buffer concentration and pH, normally in mM range) is not significantly influenced by the ion-exchange process. So eq. 7 can be

simplified by substituting: $\frac{k_{+1}k_{+2}k_{+3}}{k_{-1}k_{-2}[M^+]^2_{soln} + k_{-1}k_{+3}[M^+]_{soln} + k_{+2}k_{+3}} = k_A$ and

$\frac{k_{-1}k_{-2}k_{-3}[M^+]^3_{soln}}{k_{-1}k_{-2}[M^+]^2_{soln} + k_{-1}k_{+3}[M^+]_{soln} + k_{+2}k_{+3}} = k_B$ into it.

The rate law of the rate control reaction (3) is then given in eq. (8):

$$\frac{d\Gamma_t}{dt} = k_A[(DNA \cdot 3M^+)_{surf}]_t[Ru^{3+}]_{soln} - k_B\Gamma_t \quad (8)$$

in eq. (8), k_A and k_B are apparent rate constants for the adsorption (binding) and dissociation processes; therefore, the equilibrium constant is $K = k_A / k_B$, and the subscript t identifies a time-dependent quantity. The quantity of the surface-bound monocations at any time can be expressed as:

$$[(DNA \cdot 3M^+)_{surf}]_t = \Gamma_{sat} - \Gamma_t \quad (9)$$

Substituting eq. (9) into eq. (8) results in:

$$\frac{d\Gamma_t}{dt} = k_A[Ru^{3+}]_{soln}(\Gamma_{sat} - \Gamma_t) - k_B\Gamma_t \quad (10)$$

When at equilibrium, eq. (8) yields

$$k_A[Ru^{3+}]_{soln}(\Gamma_{sat} - \Gamma_{eq}) = k_B\Gamma_{eq} \quad (11)$$

where $\Gamma_{eq} \equiv [DNA \cdot Ru^{3+}]$ and $\Gamma_{sat} = \Gamma_{eq} + [DNA \cdot 3M^+]_{surf}$.

A rearrangement of eq. (11) gives

$$\frac{k_A}{k_B} = \frac{\Gamma_{eq}}{(\Gamma_{sat} - \Gamma_{eq})[Ru^{3+}]_{soln}} \quad (12)$$

$$k_A[Ru^{3+}]_{soln}\Gamma_{sat} = k_B\Gamma_{eq} + k_A[Ru^{3+}]_{soln}\Gamma_{eq} \quad (13)$$

By substituting eq. (13) into eq. (10), eq. (14) results

$$\frac{d\Gamma_t}{dt} = k_B\Gamma_{eq} + k_A[Ru^{3+}]_{soln}\Gamma_{eq} - k_A[Ru^{3+}]_{soln}\Gamma_t - k_B\Gamma_t \quad (14)$$

A rearrangement of eq. (14) gives eq. (15)

$$\frac{d\Gamma_t}{dt} = (k_A[Ru^{3+}]_{soln} + k_B)(\Gamma_{eq} - \Gamma_t) \quad (15)$$

When an initially prepared gold electrode modified with a thiolate-DNA monolayers is placed in a solution containing the $[Ru(NH_3)_6]^{3+}$ complex, integration of eq. (15) leads to

$$\ln(1-\theta) = -k_{app}t \quad (16)$$

where θ is the surface coverage and k_{app} is the apparent first-order rate constant which are given by eq. (17) and eq. (18) respectively

$$\theta = \frac{\Gamma_t}{\Gamma_{eq}} = \frac{Q_t}{Q_{eq}} \quad (17)$$

$$k_{app} = k_A[Ru^{3+}]_{soln} + k_B \quad (18)$$

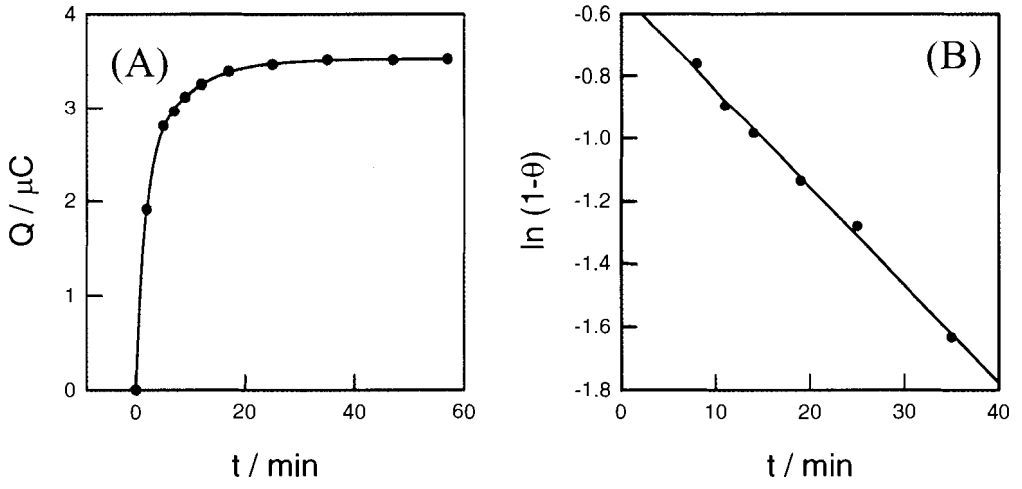

Figure 2-2 **(A) Integrated charge of the cathodic peaks from the CVs of 0.5 μM $[Ru(NH_3)_6]^{3+}$ onssDNA/Au (Figure 2-1A) as function of incubation time. (B) Plot of ln $(1-\theta)$ *versus* incubation time, from which the apparent first-order rate constant (k_{app}) was determined.**

Figure 2-2A shows the dependence of Q_t on the incubation time (t) for ssDNA/Au. As indicated by the CV curves in Figure 2-1A, the surface charge initially increases monotonically and reaches equilibrium after about 40 min. The plot of ln $(1 - \theta)$ *vs.* t shown in Figure 2-2B is linear, demonstrating the validity of eq. (16). Moreover, the apparent first-order rate constant, k_{app}, can be obtained from the slope of the ln $(1 - \theta)$ *vs.* t plot (Figure 2-2B).

Table 2-1 lists the apparent first-order rate constants for the interaction of $[Ru(NH_3)_6]^{3+}$ with ssDNA/Au and dsDNA/Au at different concentrations of $[Ru(NH_3)_6]^{3+}$. Two conclusions are evident: (1) The rate constants are clearly dependent on the solution concentration; (2) the rate constant obtained for dsDNA/Au is much smaller than that of ssDNA/Au (at the same concentration of redox cations), which

indicates that the kinetics of ion-exchange binding is directly related to the structural nature of the DNA monolayers.

Table 2-1 Kinetic data for $[Ru(NH_3)_6]^{3+}$ binding to thiolate-DNA monolayers on gold.[a]

System	C_{Ru} (μM)	k_{app} (10^{-2} min^{-1})[b]
ssDNA/Au	0.30	6.0
ssDNA/Au	0.50	9.0
dsDNA/Au	0.50	1.5
dsDNA/Au	2.5	6.0
dsDNA/Au	5.0	14

[a] The surface densities (Γ_{DNA}) of ssDNA/Au and dsDNA/Au are (4.4±0.5) $\times 10^{12}$ and (4.3±0.4)$\times 10^{12}$ molecules/cm^2, respectively. The experiments were carried out in 10 mM Tris buffer at pH 7.4 at room temperature (25 °C). The ssDNA/Au and its complimentary strand have the structures Au-S-C6-5'TCGATCTGACGTCAGCT-AAA3' and 5'TTTAGCTGACGTCAGATCGA3', respectively. [b] Uncertainties are ±15%.

Pang and Abruna[1] briefly addressed the binding kinetics of benzyl viologen (BV) to calf-thymus DNA adsorbed on gold surfaces. They employed a one-term rate law instead of eq. (16) by assuming that the solution concentration remains constant and neglecting the dissociation process. At higher redox cation concentrations (10 μM BV), the "pseudo-first-order" binding rate constants they reported were 2.5×10^{-2} and 5.1×10^{-2} min^{-1} for dsDNA/Au and ssDNA/Au, respectively, i.e., smaller but of the same order of magnitude as those obtained in our study. A direct comparison is inadequate due to the different types of cations (with different charge and structure) and the different

preparation of the DNA-modified surfaces. From their values of k_A (2.5×10^3 and 5.1×10^3 $M^{-1}\cdot min^{-1,}$ calculated from their data) and K (2.0×10^4 M^{-1} and 3.6×10^4 M^{-1}), k_B can be calculated to be 8.0×10^{-2} min^{-1} for dsDNA/Au and 7.0×10^{-2} min^{-1} for ssDNA/Au. These values are even larger than the "pseudo-first-order" binding rate constants, $k' = k_A C$, i.e., the dissociation process is certainly not negligible.

2.3.2 Evaluation of the Binding Rate Constants

The second-order rate constants k_A were calculated by using eq. (9). The concentration of monocations (mainly $Tris^+$) in the solution is 8.8 mM (10 mM Tris·HCl, pK_a = 8.3) as determined from the pH value (7.4). The concentration of $[M^+]_{soln}$ remains constant during the reaction as the concentration of monocation is not significantly influenced by the ion-exchange process. As shown in Figure 2-3, the plot of k_{app} *vs.* C_{Ru} is linear, indicating the validity of eq. (18). More importantly, the second-order binding rate constants, k_A can be determined from the slope of the plot shown in Figure 2-3. The values for k_A, calculated are $2.2\pm0.3\times10^4$ $M^{-1}min^{-1}$ for dsDNA/Au and $1.3\pm0.2\times10^5$ $M^{-1}min^{-1}$ for ssDNA/Au respectively. The binding rate constant obtained for dsDNA/Au is much smaller than that of ssDNA/Au, which indicates that the binding kinetics is directly related to the structure of DNA monolayer.

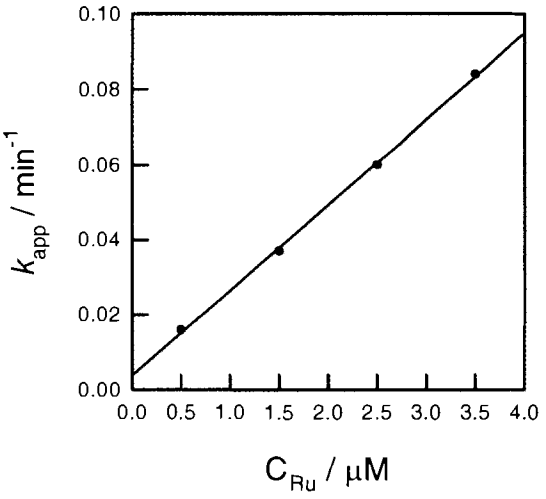

Figure 2-3 A plot of k_{app} *vs.* the concentration of $[Ru(NH_3)_6]^{3+}$ in solution for dsDNA/Au, from which the k_A was determined. See text for details.

2.3.3 Determination of the Dissociation Rate Constants

We have also examined the process of dissociation of metal cations from thiolate-DNA monolayers on gold. A simple approach to obtain dissociation rate constants consists of incubating the DNA-modified electrode in relatively concentrated $[Ru(NH_3)_6]^{3+}$ solution (e.g., 5.0 μM) and then transferring it into a redox cation-free buffer for voltammetric measurements. A similar method was used by Tarlov and co-workers to confirm that the CV postwaves were due to surface-confined species.[7b] Figure 2-4 shows that the redox peaks decrease gradually with time due to the dissociation of $[Ru(NH_3)_6]^{3+}$ from the electrode surface into the electrolyte solution.

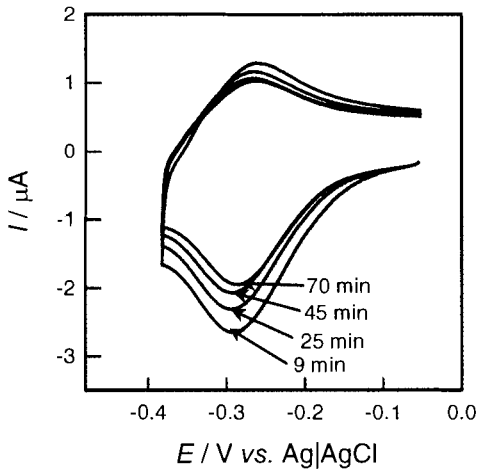

Figure 2-4 Cyclic voltammograms of dsDNA/Au in 10 mM Tris buffer at pH 7.4. The scan rate is 50 mV/s. The electrode was incubated in 5.0 μM $[Ru(NH_3)_6]^{3+}$ for 30 min before transfer into the redox-cation-free buffer.

In this case, the binding (re-adsoprtion) process is virtually non-existent, and integration of eq. (8) gives

$$\ln\theta = -k_B t \qquad (19)$$

As expected, the integrated cathodic charge, Q_t, decreases monotonically with time (Figure 2-5A). The value of k_B can be obtained from the slope of the linear portion of the $\ln\theta$ vs. t plot (Figure 2-5 B). Another approach to obtain the value of k_B is from the intercept of the plot in Figure 2-3. The obtained values were all listed in Table 2-2 for comparison.

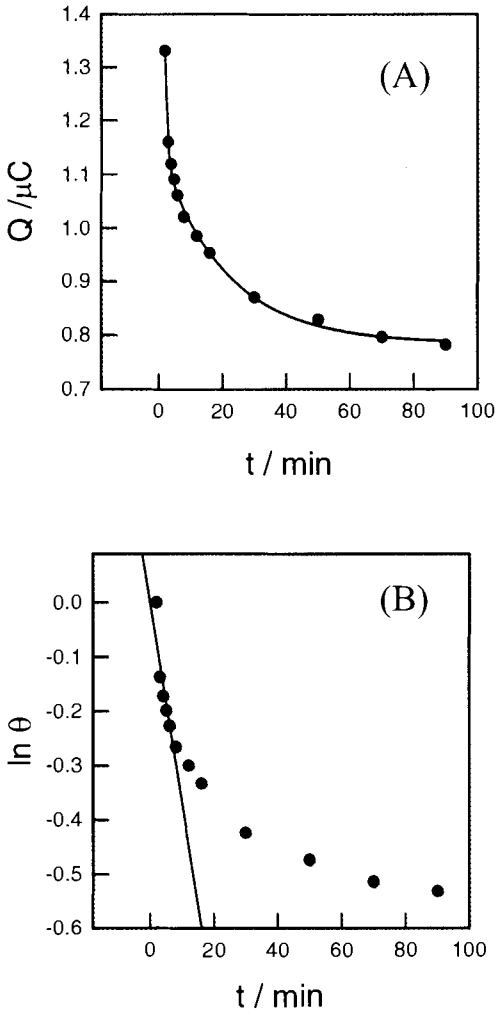

Figure 2-5 **(A) Integrated charge of the cathodic peak for $[Ru(NH_3)_6]^{3+}$ bound to dsDNA/Au as function of time after transfer to redox-free buffer. (B) Plot of ln θ as function of time, from which the dissociation rate constant (k_B) was obtained.**

The k_B values obtained from both methods are very close to each other. The value of k_B for dsDNA/Au is much smaller than that for ssDNA/Au (Table 2-2), but they are typically of the same order of magnitude (10^{-2} min^{-1}) as the apparent first-order rate constants obtained previously (Table 2-1) and dependent on the surface density of DNA strands.

Table 2-2 Rate constants for $[Ru(NH_3)_6]^{3+}$ dissociation from thiolate-DNA monolayers on gold.[a]

System	k_B (10^{-2} min^{-1})[b]	k_B (10^{-2} min^{-1})[c]
dsDNA/Au	0.4 ± 0.1	0.6±0.2
ssDNA/Au	2.2 ± 0.3	2.6±0.3

[a.] The surface densities (Γ_{DNA}) of dsDNA/Au and ssDNA/Au are 2.9×10^{12} and 4.6×10^{12} molecule / cm^2 respectively; [b.] Obtained by fitting k_{app} vs. C_{Ru} (Figure 2-3); [c.] Determined by voltammetric measurements after transfer into the redox-free buffer.

Substitution of $K = k_A / k_B$ into eq. (18) leads to

$$K = \frac{k_A}{k_B} = \frac{k_{app} - k_B}{k_B[Ru^{3+}]_{soln}} \tag{20}$$

in which $[Ru^{3+}]_{soln}$ is the concentration of the complex employed in the experiment leading to k_{app}. For the ion-exchange binding of $[Ru(NH_3)_6]^{3+}$ to ssDNA/Au, k_{app} = 6.0×10^{-2} min^{-1} (Figure 2-2), k_B = 2.7×10^{-2} min^{-1} (Figure 2-5), and $[Ru^{3+}]_{soln}$ = 0.3μM. From these three values one obtains $K = 4.1\pm0.6\times10^6$ M^{-1} which is close to the K ($1.5\pm0.5 \times 10^6$ M^{-1}) calculated from the intercept of the linearized isotherm reported previously.[8] We believe that "pure" electrostatic interaction between the metal cations and the DNA phosphate backbone limits the maximum adsorption quantity (determined by the surface density of the DNA strands and the number of bases in each strand) and localizes the binding sites. Because of the ion-exchange nature, the energy for adsorption may not depend on the surface quantity of transition metal cations.

We also observed that at high concentration of monocations (K^+) or dications (Ca^{2+} and Mg^{2+}), the dissociation rates become much faster. Immersion in 1.0 M NaCl removes *all* the $[Ru(NH_3)_6]^{3+}$ in less than 30 min, as evidenced by the total disappearance of the redox peaks. This confirms the reversibility of the electrostatic interaction between metal cations and DNA monolayers on gold; more importantly, it ensures the reusability of the DNA-modified electrodes for further studies. Detailed studies of the ion-exchange properties of several bioactive cations (K^+, Ca^{2+}, and Mg^{2+}) will be covered in Chapter 4.

2.3.4 Correlation between Binding Kinetics and DNA Surface Density

To better understand the dependence of the binding kinetics on the structure of the DNA monolayers, we adapted the approach of Herne and Tarlov[12] by controlling the deposition time to achieve varied surface densities. Changing the deposition time from 1 min to 24 h resulted in surface densities ranging from 1.8×10^{12} to 6.2×10^{12} molecules/cm^2 for ssDNA/Au, and from 2.0×10^{12} to 4.3×10^{12} molecules/cm^2 for dsDNA/Au. The apparent first-order rate constants for $[Ru(NH_3)_6]^{3+}$ binding to these DNA-modified gold electrodes were obtained at the same solution concentration (0.5 μM) from the respective cyclic voltammograms and are shown in Figure 2-6.

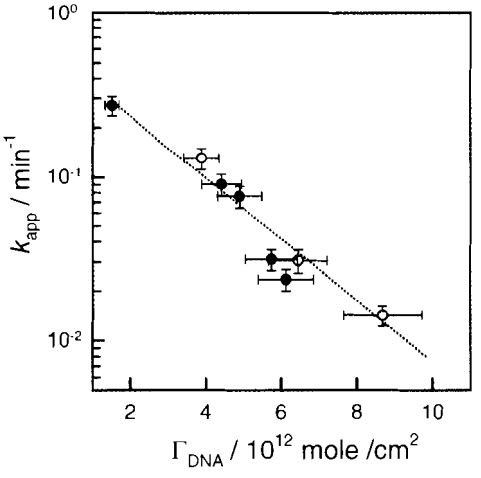

Figure 2-6 Apparent first-order rate constants of $[Ru(NH_3)_6]^{3+}$ binding to thiolate-DNA monolayers as a function of the surface density. The Γ_{DNA} values for dsDNA/Au (open circles) were doubled for direct comparison with those of ssDNA/Au (closed circles). The dashed line is to direct the eyes only.

For both ssDNA/Au and dsDNA/Au, the rate constant (k_{app}) decreases significantly as the surface density of DNA strands increases. It should be noted that, in Figure 2-6, the Γ_{DNA} values (molecules/cm^2) measured for dsDNA/Au were doubled in order to compare the density of single DNA strands directly. In both cases, the decreases follow a similar trend, indicating insignificant differences in the kinetics of cation binding to ssDNA/Au and dsDNA/Au. Atomic force microscopic (AFM) studies confirmed that bulk DNA adsorbed on solid substrates (e.g., ϕ×174 double-stranded plasmid DNA on mica) display random super-coiled morphologies, with surface coverage depending on sample load and surface treatment procedure.[13] In contrast, thiolate-DNA strands (e.g., 6-mercaptohexyl-oligonucleotides) strongly bind to gold;[14] particularly the thiolate-dsDNA oligonucleotides form well-packed monolayers with an average 45° orientation of the helical axis with respect to the surface.[14b] Recent studies by

Steel at al. have confirmed that adsorbed thiol-ssDNA oligonucleotides shorter than 24 bases *also* organize in end-tethered, highly extended configurations that allow the formation of equilibrated, close-packed monolayers.[15] We believe that the observed sluggish kinetics is due to the close proximity of the parallel DNA chains, leaving only narrow channels for the movement of metal ions. This hinders the penetration of $[Ru(NH_3)_6]^{3+}$ into the DNA monolayer and the ejection of M^+, although thermodynamically the reaction is favorable (as evidenced by the large binding constant $K = 2.0 \pm 0.5 \times 10^6\ M^{-1}$ for dsDNA/Au[8]).

2.4 Conclusions

The present study demonstrates that the simple voltammetric protocol is capable of monitoring the kinetics of the interaction of multiply charged transition metal cations with thiolate-DNA monolayers on gold. Rate constants can be obtained by integration of the rate laws based on the time-dependent voltammetric behaviors of the surface-bound redox metal cations. Our experimental results showed that the kinetics of ion-exchange binding of transition metal cations to thiolate-DNA monolayers is highly dependent on the DNA surface density, and appears to agree with the model of conventional Langmuir adsorption.

2.5 References

1. Pang, D.W.; Abruña, H. D. *Anal. Chem.* **2000,** *72*, 4700-4706.
2. Tirado, J. D.; Acevedo, D.; Bretz, R. L.; Abruña, H. D. *Langmuir* **1994**, *10*, 1971-1979.
3. (a) Campbell, J. L. E.; Anson, F. C. *Langmuir* **1996**, *12*, 4008-4014. (b) Bhugun, I. Anson, F. C. *J. Electroanal. Chem.* **1997**, *439*, 1-6.
4. Hu, K.; Bard, A. J. *Langmuir* **1998**, *14*, 4790-4794.
5. Bourdillon, C.; Demaille, C.; Moiroux, J.; Savéant, J.-M. *J. Am. Chem. Soc.* **1999**, *12*, 2401-2408.
6. Aslanoglu, M.; Isaac, C. J.; Houlton, A.; Horrocks, B. R. *Analyst* **2000,** *125*, 1791-1798.
7. (a) Steel, A. B.; Herne, T. M.; Tarlov, M. J. *Anal. Chem.* **1998**, *70*, 4670-4677. (b) Steel, A. B.; Herne, T. M.; Tarlov, M. J. *Bioconjugate Chem.* **1999**, *10*, 419-423.
8. Yu, H. Z.; Luo, C. Y.; Sankar, C. G.; Sen, D. *Anal. Chem.* **2003,** *75*, 3902-3907.
9. Rudisser, S.; Tinoco, Jr., I. *J. Mol. Biol.* **2000**, *295*, 1211-1223.
10. Maguire, J. L.; Collins, R. A. *J. Mol. Biol.* **2001**, *309*, 45-56.
11. (a) Oyama, N.; Shimomura, T.; Shigehara, K.; Anson, F. *J. Electroanal. Chem.* **1980**, 112, 271-280. (b) Oyama, N.; Anson, F. C. *Anal. Chem.* **1980**, *52*, 1192-1198. (c) Shigehara, K.; Oyama, N.; Anson, F. C. *J. Am. Chem. Soc.* **1981**, *103*, 2552-2558.
12. Herne, T. M.; Tarlov, M. J. *J. Am. Chem. Soc.* **1997**, *119*, 8916-8920.
13. (a) Umemura, K.; Ishikawa, M.; Kuroda, R. *Anal. Biochem.* **2001**, *290*, 232-237. (b) Auman, K.; Muyskens, K. J. C.; Sinniah, K. *J. Chem. Educ.* **2003**, *80*, 187-183.
14. (a) Rekesh, D.; Lyubchenko, Y.; Shlyakhtenko, L. S.; Lindsay, S. M. *Biophys. J.* **1996**, *71*, 1079-1086. (b) Kelley, S. O.; Barton, J. K.; Jackson, N. M.; McPherson, L. D.; Potter, A. B.; Spain, E. M.; Allen, M. J.; Hill, M. G. *Langmuir* **1998**, *14*, 6781-6784. (c) Ceres, D. M.; Barton, J. K. *J. Am. Chem. Soc.* **2003**, *125*, 14964-14965.
15. Steel, A. B.; Levicky, R. L.; Herne, T. M.; Tarlov, M. J. *Biophys. J.* **2000**, *79*, 975-981.

CHAPTER 3
VOLTAMMETRIC SENSING OF METAL CATIONS BASED ON THEIR ION-EXCHANGE BINDING TO DNA-MODIFIED SURFACES

This chapter describes a quantitative detection of non-electroactive ions by the simple electrochemical protocol, specifically mono- and divalent metal cations of biological relevance (Mg^{2+}, Ca^{2+}, and K^{+}), based on their competitive binding to DNA-modified surfaces. In addition to shed light on the quantitative understanding of interactions between divalent cations and DNA-modified surface, the equilibrium binding constants were also calculated.

3.1 Introduction

In the second chapter and previous publications from our group, we have reported an electrochemical procedure to examine DNA-modified surfaces, i.e., to quantitate the density of DNA probes on chips and to monitor the heterogeneous hybridization with target strands in solution (see chapter 1).[1] In this chapter, we demonstrate that this method can be extended to the quantitative analysis of non-electroactive metal cations, such as magnesium (Mg^{2+}), calcium (Ca^{2+}), and potassium (K^{+}). These metal cations are of particular biological importance;[2] for example, they play a crucial role in the human body, i.e., small deviations from normal concentration levels are recognized as symptoms of malfunction or disease.

In the past, very few electrochemical or optical sensors have been found to be suitable for the detection of these bioreactive metal cations, particularly for Mg^{2+}.[3] This is partially due to the limited availability of host compounds, either synthetic or naturally existing, that bind Mg^{2+} in preference to other alkali and alkaline earth metal ions. Almost a decade ago, Meada and co-workers proposed to use double-helical DNA (chemisorption of disulfide-tethered-calf thymus DNA on gold) as receptive entity for the detection of Mg^{2+}, by monitoring the enhanced signal of ferrocyanide/ferricyanide ($[Fe(CN)_6]^{3-/4-}$) redox couple on DNA-modified electrodes upon adding Mg^{2+}.[4] The same approach was used to detect other metal cations (Ca^{2+}, K^+, and Na^+)[4] and even anti-cancer drugs.[5] Without exploring the sensing perspectives, several other groups reported the effect of ionic strength (essentially the concentration of mono- or divalent metal ions in the electrolyte solution) on the electrochemical behavior of redox-active molecules on electrodes modified with DNA strands.[6-10] For example, Pang and Abruña reported that with increased concentrations of NaCl in the supporting electrolyte, the peak currents and potentials of $[Co(Phen)_3]^{3+/2+}$ (Phen = 1,10-phenanthroline) decreased / shifted significantly.[9a] This allowed them to discuss various interaction modes between redox cations and DNA strands on electrode surface.[9]

To date, most of the reported electrochemical DNA sensors are directed toward applications in genetic screening and detection, i.e., to identify selected DNA sequences or mutated genes associated with human disease.[11] Different laboratories are just starting to take advantage of the ease of DNA sensor design for the development of assays for other molecular analytes (from small molecules to proteins) that bind to DNA. For example, Ozsoz et al. recently reported the detection of arsenic trioxide, by monitoring

the direct guanine oxidation.[12] Based on the DNA-mediated charge transport chemistry, Barton and co-workers developed an electrochemical protocol to assay for protein (e.g., M.*HhaI*, a base-flipping enzyme) binding to and reacting with DNA-modified surfaces.[13] Kraatz and co-workers demonstrated that the binding event of MutS protein to a double-stranded DNA containing a single nucleotide mismatch can be conveniently detected by electrochemical impedance spectroscopy.[14] Along the same line of exploration, the present work stems from our continued efforts to develop versatile electrical DNA sensors for molecular analytes by constructing conformational DNA-switches.[15] This report represents our first step in exploring electrochemical DNA/RNA-binding assays for more specific biomedical analytes, by demonstrating that a simple voltammetric protocol in conjunction with DNA-modified electrodes can be used to detect the presence of different types of metal cations at low concentrations.

3.2 Experimental Section

Detailed experimental procedures for the purification and surface-immobilization of synthetic DNA strands have been reported previously (see chapter 2). In brief, the disulfide-modified oligonuleotide, DMT-O-$(CH_2)_6$-S-S-$(CH_2)_6$-O-5'TCGATCTGAC-GTCAGCTAAA3' (Core DNA Services Inc., Calgary, AB) was treated with saturated $NH_3 \cdot H_2O$ at 55 °C for 12 h to deprotect the bases and the DNA sample was purified by reversed phase HPLC on a C18 Vydac Column (218TP54). After reacting with 100 mM DTT (dithiothreitol) at pH 8.5 for 30 min (to break the disulfide bond), the resulting thiol-terminated oligonucleoide, $HS(CH_2)_6$O-5'-TCGATCTGACGTCAGCTAAA3' (HS-ssDNA), was purified and desalted on a Pharmacia Nap-5 Column (G-25 Sephadex). To prepare double-stranded oligonucleotides (dsDNA), we hybridized a 10 μM solution of

HS-ssDNA with the complimentary strand (5'TTTAGCTGACGTCAGATCGA3') in deoxygenated buffer (10 mM Tris containing 0.1 M $MgCl_2$ and 1 M NaCl at pH 7.4) by heating to 90 °C, followed by slowly cooling down to room temperature.

Glass slides coated with 10 nm Ti and 100 nm Au (Evaporated Metal Film, Inc., Ithaca, NY) (1.5 × 2.5 cm^2) were cleaned by immersion in a mixture of concentrated sulfuric acid and hydrogen peroxide (3:1, v/v) for 2 to 5 min at 90 °C. They were then rinsed thoroughly with deionized water and dried under N_2. To prepare gold electrodes modified with double-stranded DNA (dsDNA/Au), we spread 100 μL of a 10 μM solution of the dsDNA over the cleaned gold surface for 24 h at ambient conditions. After the modification, the electrode was rinsed with 10 mM Tris buffer solutions containing 50 mM and 10 mM NaCl, respectively, and subsequently immersed in a 1.0 mM 6-mercapto-1-hexanol (MCH) solution for 10 min. The resulting sample was cleaned with 10 mM Tris buffer solution and dried under N_2 before characterization.

Electrochemical measurements were carried out using a μAutolab II potentiostat (Eco Chemie B.V., Utrecht, Netherlands). A gold slide modified with double-stranded DNA (dsDNA/Au) was used as the working electrode; it was pressed against an O-ring seal at the Teflon cell bottom with an exposed area of 0.68 cm^2. An Ag | AgCl | 3.0 M NaCl electrode was used as reference electrode, and the counter electrode was a Pt coil. The electrolyte and buffer solutions were prepared with deionized water (>18.3 MΩ·cm; Barnstead EasyPure UV/UF compact water system, Dubuque, IA) and chemicals of ACS reagent grade, unless otherwise stated.

3.3 Results and Discussions

As confirmed previously by electrochemical[1a,16] and atomic force microscopic (AFM) measurements,[17] thiol-tethered dsDNA strands form densely packed and uniform monolayers on gold surfaces with a surface density as high as $(4.6\pm0.6) \times 10^{12}$ molecules/cm.[1a,11] Subsequent treatment in a dilute solution of MCH improves the quality of the monolayers by backfilling the unmodified gold surfaces and projecting the DNA strands into solution. When the modified gold electrodes are exposed to an aqueous solution of $Ru(NH_3)_6Cl_3$, a multiply charged transition metal complex, at low ionic strength, an ion-exchange equilibrium between the redox cations and the native charge compensation monovalent cations ($Tris^+$ or Na^+) associated with the anionic DNA backbone is established (Figure 3-1).[1, 18] This process may take several tens of minutes, depending on the surface density of the dsDNA strands and the concentration of redox cations.[1b] To facilitate the equilibration, we used the highest concentration possible (if the

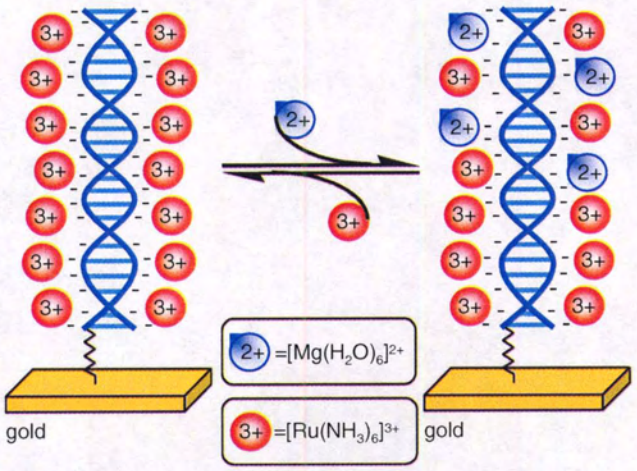

Figure 3-1 Pictorial illustration of the ion-exchange binding of Mg^{2+} (in the form of $[Mg(H_2O)_6]^{2+}$) to a dsDNA-modified gold electrode that has been incubated in a dilute solution of $[Ru(NH_3)_6]^{3+}$.

concentration is too high, diffusion peaks show up, which influence the calculation accuracy)[1a] and made sure that the electrode has been incubated for a sufficiently long time period.[1b] Based on the charge (Q) obtained by integrating the cathodic peak in the cyclic voltammogram (Figure 3-2), the surface concentration of redox cations ($\Gamma_{Ru\cdot DNA/Au}$) that are electrostatically bound to the DNA strands can be determined,[1]

$$Q_{sat} = nFA\Gamma_{Ru\cdot DNA/Au} \qquad (1)$$

where n is the number of electrons involved in the redox reaction, F is the Faraday constant, and A is the area of the working electrode. Under the condition of saturation (determined from the adsorption isotherm), the surface density of DNA can be directly calculated from $\Gamma_{Ru\cdot DNA/Au}$, as reported previously.[1a] It is used here as a simple quality control of the modified electrode before further experiments are carried out.

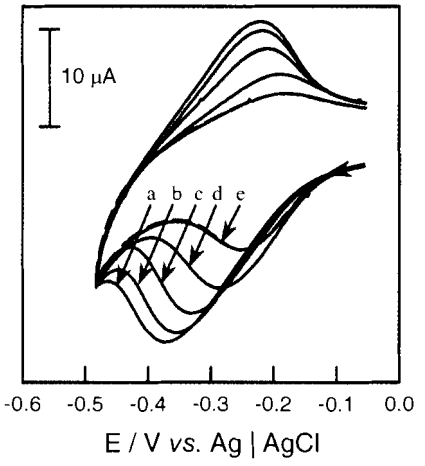

Figure 3-2 **Cyclic voltammograms of 5.0 μM $[Ru(NH_3)_6]^{3+}$ on dsDNA/Au upon increasing the concentration of Mg^{2+} in the supporting electrolyte. The electrolyte was 10 mM Tris buffer at pH 7.4, and the scan rate was 300 mV/s. From curve a to e, the corresponding concentration of Mg^{2+} are 0, 40, 100, 300, and 800 μM. The dashed lines show the "steady-state" CV, i.e., the CV recorded at a high concentration of Mg^{2+} (1.0 mM) beyond which no further changes are observed.**

These experiments were normally carried out in a buffer of low ionic strength and without additional supporting electrolyte (typically 10 mM Tris). After incubation in 5.0 μM $[Ru(NH_3)_6]^{3+}$ for more than 30 min, clear reduction and oxidation peaks due to the surface-bound redox cations are observed, as shown in Figure 3-2(curve a). The separation between the two peaks is more than 100 mV at a scan rate of 300 mV/s, which is due to the expected slow electron-transfer kinetics.[1a] The most striking observation here is the variation of these redox peaks upon adding other metal cations. Figure 3-2 (curve b to e) shows the sequential changes when the concentration of Mg^{2+} added to the electrolyte solution increases from 40 μM to 0.8mM. The peak currents decrease significantly, and the positions of both anodic and cathodic peaks shift toward the positive direction. It should be noted that these changes are reversible, i.e., after washing the electrode with 1M NaCl solution and incubation in 10 mM Tris buffer solution, the results can be reproduced with the same electrode.

Since the peak area (thus the integrated charge) is a direct measure of the concentration of surface-bound $[Ru(NH_3)_6]^{3+}$, the result shown in Figure 3-2 indicate a shift of the ion-exchange equilibrium between the redox cations and other metal cations added subsequently, as depicted in Figure 3-1. When certain amount of other metal cations is present, they essentially compete for the negatively charged phosphate-diester backbone of DNA strands. The pre-bound redox cations ($[Ru(NH_3)_6]^{3+}$) are replaced by the subsequently added non-electroactive cations, which leads to the observed decrease of the redox peak. To quantitate this effect, we have plotted the changes of the integrated charge of the cathodic peak as a function of the concentration of subsequently added metal cations (Figure 3-3).

The comparison between the three types of metal cations (Mg^{2+}, Ca^{2+} and K^{+}) examined in this study is unambiguous. The lowest Mg^{2+} concentration producing a change in the voltammetric response is approximately 10 μM, and the plot of ΔQ *vs.* log $[Mg^{2+}]$ is almost linear in the concentration range from 10 to 100 μM. For Ca^{2+}, the threshold concentration is about 10 times higher (~100 μM), and the linear region ranges from 200 to 500 μM. For K^{+}, no change was observed until the concentration reached a ~50 mM, and the signal decreased abruptly at higher concentrations. These results, particularly the threshold concentrations for different metal cations, are similar to those reported by Maeda et al,[19] by monitoring the peak current changes for the $[Fe(CN)_6]^{3-}$ /$[Fe(CN)_6]^{4-}$ couple. In comparison, our data shown in Figure 3-3 cover a much wider linear-response region for Mg^{2+} and a clearer distinction between mono- and divalent cations.

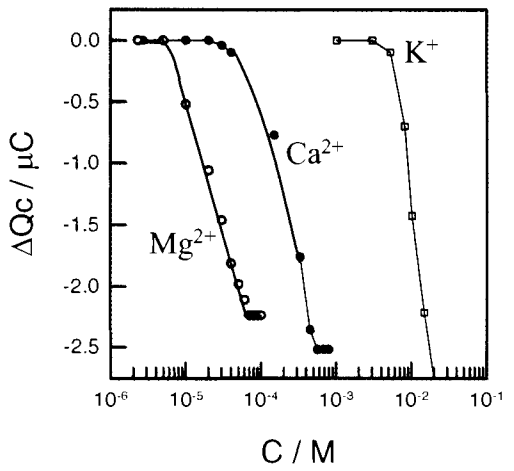

Figure 3-3 Decrease of the integrated charge of the cathodic peak in the CVs for 5.0 μM $[Ru(NH_3)_6]^{3+}$ on DNA-modified electrodes (shown in Figure 3-2) as function of the concentration of different metal cations subsequently added to the electrolyte: Mg^{2+}(○), Ca^{2+}(●), and K^{+}(□).

To further illustrate the effect of subsequently added metal cations on the voltammetric response of $[Ru(NH_3)_6]^{3+}$, we also plotted the shifts of the formal potential ($\Delta E^{\circ'}$) as function of their concentrations (Figure 3-4); the formal potential was estimated from the positions of the cathodic (E_{pc}) and anodic (E_{pa}) peaks using eq. (2).

$$E^{\circ'} = \frac{E_{pc} + E_{pa}}{2} \qquad (2)$$

It is interesting to note that Figures 3-3 and 3-4 show very similar trends, particularly for the detectable concentration ranges of the three cations. However, the changes of the formal potential indicate that the threshold concentration of Ca^{2+} could be as low as 30 μM, i.e., the two divalent cations differ much less from each other than from the monovalent ion (K^+).

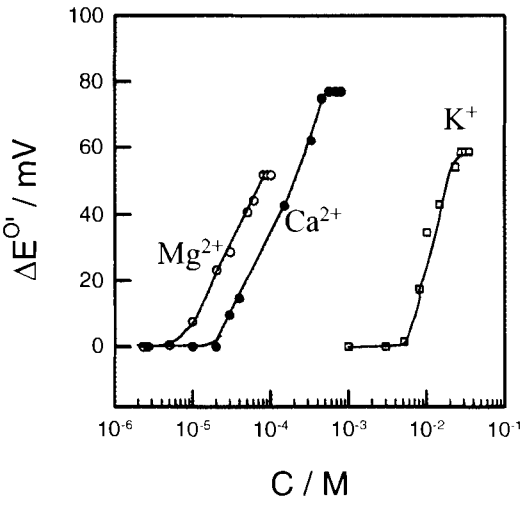

Figure 3-4 Shifts of the formal potential of 5.0 μM $[Ru(NH_3)_6]^{3+}$ on DNA-modified electrodes (shown in Figure 3-2) as function of the concentration of different metal cations subsequently added to the electrolyte: Mg^{2+}(○), Ca^{2+}(●), and K^+(□).

As has been reported previously, the interactions between DNA and redox cations depend on the ionic strength of the supporting electrolyte.[9] The validity of above method for detecting metal cations relies on the fact that the changes of the voltammetric response are *not* resulting from the variation of the ionic strength of the supporting electrolyte solution. In Figure 3-5A, we plotted the solution ionic strength as a function of the concentration of the metal cations. Because in all cases 10 mM Tris buffer solution

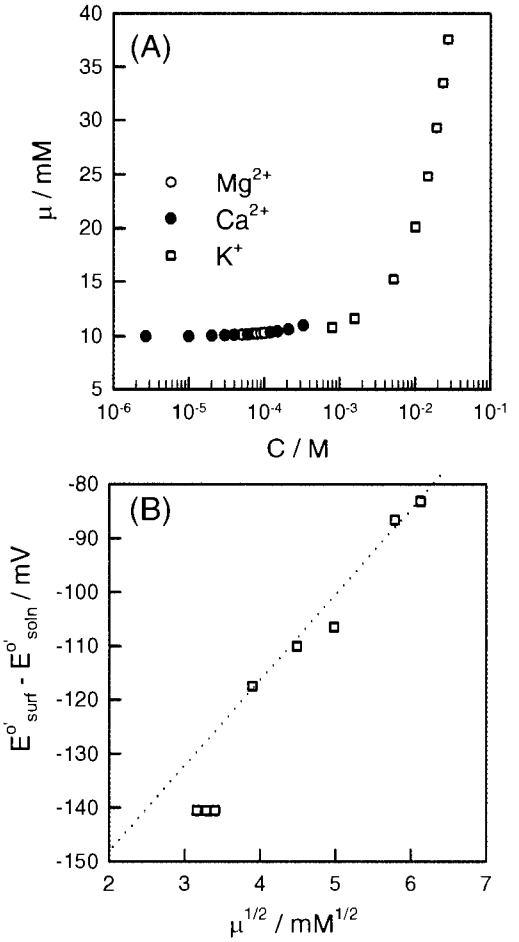

Figure 3-5 **(A) Ionic strength of the electrolyte solution as function of the concentration of the subsequently added metal cations: Mg^{2+}(○), Ca^{2+}(●), and K^{+}(□). (B) Difference between the formal potentials of surface-confined and solution-diffused $[Ru(NH_3)_6]^{3+}$ versus the ionic strength of the electrolyte solution at different concentrations of K^{+}.**

was used (minimum requirement for conductivity), the ionic strength did not change significantly in the experiments with Mg^{2+} and Ca^{2+}, as their concentrations were much lower (in the μM or sub-mM ranges). This suggests that the voltammetric signal changes on addition of these two cations are not due to changes of the ionic strength.

In the case of K^+, the ionic strength increases significantly in the tested concentration range (Figure 3-5A), which raises the question whether the mode of cation-DNA binding varies. Pang and Abruña suggested the binding mode of redox cation, $[(Co(Phen)_3]^{3+}$, to dsDNA could change from electrostatic to intercalative when the ionic strength of the solution is increased.[9]

$$\begin{array}{ccc} [Ru(NH_3)_6]^{3+}_{soln} + e^- & \overset{E^{\circ'}_{soln}}{\rightleftharpoons} & [Ru(NH_3)_6]^{2+}_{soln} \\ \Big\updownarrow K_{3+} & & \Big\updownarrow K_{2+} \\ [Ru(NH_3)_6]^{3+}_{surf} + e^- & \overset{E^{\circ'}_{surf}}{\rightleftharpoons} & [Ru(NH_3)_6]^{2+}_{surf} \end{array}$$

Figure 3-6 General process (a square scheme) of the binding of $[Ru(NH_3)_6]^{3+}$ to a DNA-modified surface. The subscripts surf and soln denote the surface-bound and solution-diffused species, respectively.

The general process of metal cations binding to DNA strands can be described by a square scheme proposed initially by Carter et al.[6b] In this diagram (Figure 3-6), the difference in the formal potential of surface-confined ($E^{\circ'}_{surf}$) and solution-diffused ($E^{\circ'}_{soln}$) species can be described as:

$$E^{\circ'}_{surf} - E^{\circ'}_{soln} = -\frac{RT}{nF}\ln\left(\frac{K_{3+}}{K_{2+}}\right) \qquad (3)$$

where K_{3+} and K_{2+} are the equilibrium binding constants for the oxidized and reduced forms, $[Ru(NH_3)_6]^{3+}$ and $[Ru(NH_3)_6]^{2+}$, respectively. As shown in Figure 3-5B, the differences between $E^{o'}_{surf}$ and $E^{o'}_{soln}$ were always negative upon increasing the ionic strength of the electrolyte solution, and the change of formal potential is approximately proportional to $\mu^{1/2}$.[9] This indicates that the oxidized form, $[Ru(NH_3)_6]^{3+}$, binds to the DNA-modified surface more strongly than the reduced form, $[Ru(NH_3)_6]^{2+}$, i.e., K_{3+} is larger than K_{2+}, which is characteristic for electrostatic interactions.[9a] The result shown in Figure 3-5 confirms that over the entire concentration range tested, the interactions between $[Ru(NH_3)_6]^{3+}$ and DNA are electrostatic i.e., the nature of the interaction between redox cations and dsDNA strands does not change.

It has been shown previously that the equilibrium binding constant for the interaction between redox metal cations and DNA-modified surfaces can be obtained by analysis of the adsorption isotherm (the integrated charge of the surface-confined redox cations as a function of their solution concentrations).[1, 18] The evaluation of the binding constants of mono- and divalent metal cations that are not electroactive, has been relying on more sophisticated techniques, such as NMR, Electron Paramagnetic Resonance, or X-ray diffraction measurements.[2, 20-21] We propose here, based on the voltammetric signal changes of the pre-bound redox cations upon adding non-electroactive metal cations (for example, Mg^{2+} and Ca^{2+}), to determine their binding constants to DNA-modified surfaces. Specificlly, the decrease of the integrated charge is a measure of the extent to which other cations compete or interfere with the binding of $[Ru(NH_3)_6]^{3+}$ to DNA. The determination of the binding constants of Mg^{2+} and Ca^{2+} is also based on the Langmuir model (eq. 4),

which assumes that every binding site is equivalent and the ability of a molecule to bind is independent of the occupation of nearby sites.

$$\frac{C}{Q_{eq}} = \frac{C}{Q_{sat}} + \frac{1}{KQ_{sat}} \qquad (4)$$

where $Q_{eq} = Q_{int} - Q$ and $Q_{sat} = Q_{int} - Q_{fin}$. Q_{int} is the saturated charge of $[Ru(NH_3)_6]^{3+}$ before adding other cations, Q is the equilibrium charge of $[Ru(NH_3)_6]^{3+}$ in the presence of a certain concentration (C) of another cation, and Q_{fin} is the final charge of $[Ru(NH_3)_6]^{3+}$ beyond which it does not decrease upon increased concentration (C) of the competing cation. As shown in Figure 3-7, the experimental data for high concentrations of Mg^{2+} and Ca^{2+} fit the Langmuir model (eq. 4) well. For lower concentrations of cations, it is likely that the systems are not at equilibrium. According to eq. (7) in chapter two, both the forward and reverse rate constants will be affected by the cation concentration. The calculated equilibrium binding constants K are $6.7\pm0.5 \times 10^4$ M^{-1} and $3.8\pm0.5 \times 10^4$ M^{-1} for Mg^{2+} and Ca^{2+}, respectively. The electrochemical data obtained for K^+ do not fit this simple model, which we believe to be due to weaker binding of monocations to DNA strands on the surface particularly upon competing with pre-bound multiply charged metal transition cations $[Ru(NH_3)_6]^{3+}$.

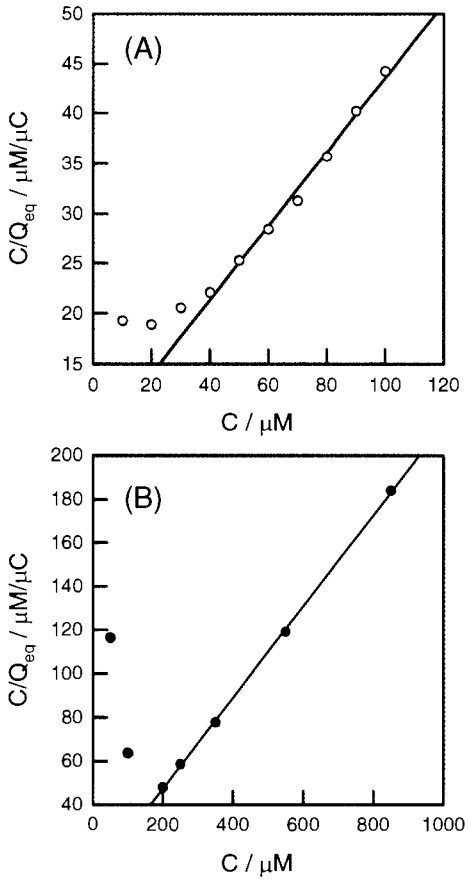

Figure 3-7 Linearized binding isotherms of Mg^{2+} (A) and Ca^{2+} (B) on DNA-modified gold electrodes based on the Langmuir model. The lines fit to the experimental data in the linear region at high concentrations of cations using the method of least-squares, from which the binding constants were determined.

It is difficult to interpret these binding constants; however, they allow a quantitative comparison of the binding abilities of metal cations to DNA-modified surfaces. Both divalent cations (Mg^{2+} and Ca^{2+}) bind more weakly than the triply charged transition metal cation (for $[Ru(NH_3)_6]^{3+}$ $K = 2.0\pm0.5 \times 10^6$ M^{-1});[1a] and Mg^{2+} binds more strongly than Ca^{2+} to surface-bound DNA. In addition, this result supports the previously reported order of relative binding capacities: $Mg^{2+} > Ca^{2+} > K^+$ [6, 21b] It has been confirmed previously with x-ray diffraction measurements that the stronger binding of

Mg^{2+} (in the form of $[Mg(H_2O)_6]^{2+}$) is due to its rigid and stable octahedral primary solvation shell.[20] In contrast, Ca^{2+} has a much more variable first solvation shell, which does influence their site-specific binding to dsDNA strands.

3.4 Conclusions

The present work has shown that, via competitive binding studies with redox transition metal cations ($[Ru(NH_3)_6]^{3+}$), DNA-modified electrodes can be used to detect and estimate the concentrations of mono- and divalent cations, including Mg^{2+}, Ca^{2+}, and K^+. The analysis can be carried out either by monitoring the integrated charge decrease or the shift of the formal potential of the pre-bound $[Ru(NH_3)_6]^{3+}$. The sensitivity decreases in the order $Mg^{2+} > Ca^{2+} > K^+$, which is consistent with their relative binding abilities to thiolate-DNA monolayers on gold. In addition, the equilibrium binding constants of these metal cations can be obtained by analyzing the voltammetric data with the help of the Langmuir model.

3.5 References

1. (a) Yu, H. Z.; Luo, C. Y.; Sankar, C. G.; Sen, D. *Anal. Chem.* **2003,** *75*, 3902-3907. (b) Su, L.; Sankar, C. G.; Sen, D.; and Yu, H. Z. *Anal. Chem.* **2004**, *76*, 5953-5959.
2. For examples of review papers regarding metal ion-DNA interactions, see, (a) Swiatek, J. *J. Coord. Chem.* **1994**, *33*, 191-217. (b) Anastassopoulou, J. *J. Mol. Strutc.* **2003**, *651*, 19-26. (c) Egli, M. *Chem. Bio.* **2002**, *9*, 277-286.
3. Eugster, R.; Gehrig, P. M.; Morf, W. E.; Spichiger, U. E.; Simon, W. *Anal. Chem.* **1991**, *63*, 2285-2289, and references cited therein.
4. Maeda, M.; Nakano, K.; Uchida, S.; Takagi, M. *Chem. Lett.* **1994**, 1805-1808.
5. Nakano, K.; Maeda, M.; Uchida, S.; Takagi, M. *Anal. Sci.* **1997**, *13*, 455-456.
6. (a) Carter, M. T.; Bard, A. J. *J. Am. Chem. Soc.* **1987**, *109*, 7528-7530. (b) Carter, M. T.; Rodriguea, M.; Bard, A. J. *J. Am. Chem. Soc.* **1989,** *111*, 8901-8911.

7. Horrocks, B. R.; Mirkin, M. V. *Anal. Chem.* **1998**, *70*, 4653-4660. (b) Aslanoglu, M.; Isaac, C. J.; Houlton, A.; Horrocks, B. R. *Analyst* **2000,** *125*, 1791-1798.

8. (a) Millan, K. M.; Mikkelsen, S. R. *Anal. Chem.* **1993,** *65*, 2317-2323. (b) Millan, K. M.; Saraullo, A.; Mikkelsen, S. R. *Anal. Chem.* **1994**, *66*, 2943-2948.

9. (a) Pang, D.W.; Abruña, H. D. *Anal. Chem.* **1998,** *70*, 3162-3169. (b) Pang, D.W.; Abruña, H. D. *Anal. Chem.* **2000,** *72*, 4700-4706.

10. Erdem, A.; Meric, B.; Kerman, K.; Dalbasti, T.; Dalbsti, T.; Ozsoz, M. *Electroanalysis* **1999**, *11*, 1372-1376.

11. For recent reviews of electrochemical detection of DNA, see: (a) Drummond, T. G.; Hill, M. G.; Barton, J. K. *Nat. Biotechnol.* **2003**, *21*, 1192-1199. (b) Vercoutere, W.; Akeson, M. *Curr. Opin. Chem. Biol.* **2002**, *6*, 816-822. (c) Fojta, M. *Electroanalysis* **2002**, *14*, 1449-1463. (d) Wang, J. *Anal. Chim. Acta.* **2002**, *469*, 63-71. (e) de-los-Santos-Álvarez, Jesús Lobo-Catañón, Miranda-Ordieres, A. J.; Tuñón-Blanco, P. *Anal. Bioanal. Chem.* **2004**, *378*, 104-118.

12. Ozsoz, M.; Erdem, A.; Kara, P.; Kerman, K.; Ozkan, D. *Electroanalysis* **2003**, *15*, 613-619.

13. Boon, E. M.; Salas, J. E.; Barton, J. K. *Nat. Biotechnol.* **2002**, *20*, 282-286.

14. Li, C. Z.; Long, Y. T.; Lee, J. S.; Kraatz, H. B. *Chem. Commu.* **2004**, 574-575.

15. Fahlman, R. P.; Sen, D. *J. Am. Chem. Soc.* **2002**, *124*, 4610-4616.

16. Kelley, S. O.; Barton, J. K.; Jackson, N. M.; Hill, M. G. *Bioconjugate Chem.* **1997**, *8*, 31-37.

17. (a) Kelley, S. O.; Barton, J. K.; Jackson, N. M.; McPherson, L. D.; Potter, A. B.; Spain, E. M.; Allen, M. J.; Hill, M. G. *Langmuir* **1998**, *14*, 6781-6784. (b) Ceres, D. M.; Barton, J. K. *J. Am. Chem. Soc.* **2003**, *125*, 14964-14965.

18. (a) Steel, A. B.; Herne, T. M.; Tarlov, M. J. *Anal. Chem.* **1998,** *70*, 4670-4677. (b) Steel, A. B.; Herne, T. M.; Tarlov, M. J. *Bioconjugate Chem.* **1999,** *10*, 419-423.

19. Maeda, M.; Nakano, K.; Uchida, S.; Takagi, M. *Chem. Lett.* **1994**, 1805-1808.

20. Subirana, J. A.; Soler-Lopez, M. *Annu. Rev. Biophys. Biomol. Struct.* **2003**, *32*, 27-45, and references therein.

21. For examples, see: (a) Bleam, M. L.; Anderson, C. F.; Record, Jr., T. R. *Proc. Natl. Acad. Sci. USA* **1980**, *77*, 3085-3089. (b) Reuben, J.; Gabbay, E. J. *Biochemistry* **1975**, *14*, 1230-1234. (c) Gao, Y. G.; Sriram, M.; Wang, H.-J. *Nucleic Acids Res.* **1993**, *21*, 4093-4101.

CHAPTER 4
ELECTROCHEMICAL DEOXYRIBOSENSOR FOR SPECIFIC DETECTION OF ADENOSINE: A PRELIMINARY STUDY

In this chapter, a deoxyribosensor incorporating both ATP/adenosine aptamer and thiol-modifier was designed and immobilized onto gold electrode through sulfur-gold linkages. The switching to an 'ON' state was detected directly by a simple electrochemical protocol in the presence of the analyte, adenosine, as evidence by the increase of cyclic voltammetric signals from the surface-bound redox cations. The binding constant for adenosine binding to the deoxyribosensor on chip was also calculated.

4.1 Overview

DNA "aptamers" are molecular receptors made of single and/or double stranded oligonucleotides, capable of specifically binding a variety of molecules including many that normally do not interact with DNA or RNA.[1] As reviewed recently by Hermann and Patel,[2] aptamers are obtained by *in vitro* selection out of large pools of random-sequence oligonucleotides, and typically bind their specified ligand by induced-fit mechanisms. In 1995, Huizenga and Szostak reported an ATP-binding DNA aptamer, which specifically bound ATP as well as adenosine.[3] High-resolution NMR studies on this aptamer revealed that it was a symmetrical bulge loop bound by two DNA double helical elements.[4] It was also found that one aptamer molecule bound two adenosines, and upon binding the aptamer's loose structure compacts to a tightly hydrogen-bonded and base-stacked helical

structure.[4] Based on this ligand-driven structural compaction of the aptamer, and on the reported ability of DNA double helices to conduct electrical charge,[5] we proposed that interruption of a DNA charge conduction path by the ATP/adenosine aptamer might generate an electrical biosensor that conducts only in the presence of bound adenosine (Figure 4-1A).[6]

However, until now charge conduction/structural change in the adenosine/ATP deoxyribosensor has been inferred only indirectly by using cumbersome biochemical protocols,[6] or by other optical methods.[7] Here we report that the aptamer-ligand binding

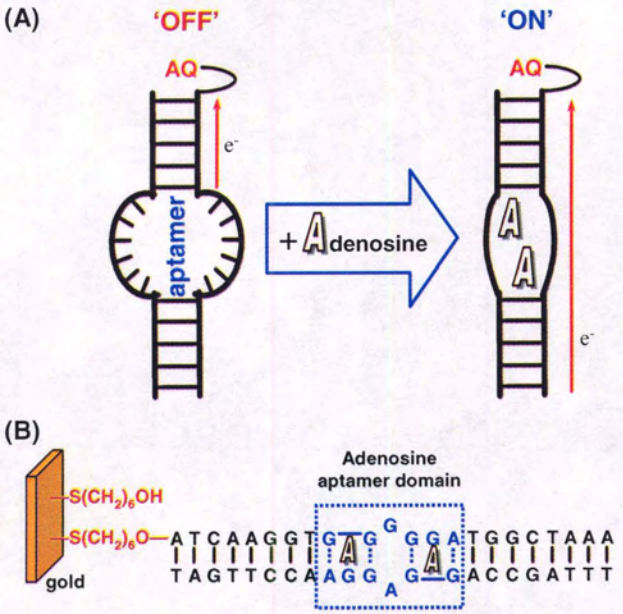

Figure 4-1 **(A) Design of a "deoxyribosensor" for the specific detection of adenosine, and the illustration of the proposed structural change upon ligand / analyte binding. (B) Modification and immobilization of such a deoxyribosensor (DNA assembly) on gold substrates for electrochemical detection. The molecules / DNA sequences are not scaled.**

event can be measured directly as an electrical output *via* the chemical coupling of the deoxyribosensor to a conductive surface (a chip). We approached this goal by immobilizing the adenosine deoxyribosensor onto a gold electrode using sulfur-gold

linkages (Figure 4-1B), with the expectation that this deoxyribosensor would progressively switch "ON" upon adenosine binding and permit direct electrochemical measurements. A simple voltammetric procedure for studying DNA-modified surfaces (including quantitation of DNA probes and monitoring of hybridization efficiency on chips) developed in our laboratories recently[8] was adapted to probe such a binding event. Our approach is based on the voltammetric response of multiply charged transition metal cations, such as $[Ru(NH_3)_6]^{3+}$, that are electrostatically bound to DNA strands. In comparison with other electrochemical methods,[9-11] this protocol offers the attractive features of experimental simplicity and ease of interpretation of the results. Micromolar concentrations (μM) of the redox cations were used to distinguish the voltammetric response of the surface-confined from that of diffusible species.[8a]

The thiol-tethered deoxyribosensor (here, incorporating an adenosine aptamer sandwiched by two short stretches of DNA duplex, and a 5'-thiol modifier, Figure 4-1B) were prepared by hybridizing 10 μM concentrations of two single-stranded oligonucleotides (ssDNA) in deoxygenated buffer. The gold electrodes were then modified by spreading 100 μL of the 10μM solution of the assembled deoxyribosensors onto the cleaned surface for 24 h at ambient conditions. To improve the quality of the DNA monolayers and to passivate the surface (reduce non-specific adsorption), these modified electrodes were further treated with a dilute solution of 6-mercapto-1-hexanol (MCH).[10]

The modified gold chips (Figure 4-1B) were then used for the electrochemical measurements. Upon prolonged incubation in an electrolyte solution containing $[Ru(NH_3)_6]^{3+}$, at low ionic strength, an ion-exchange equilibrium between the transition

metal cations and the native charge-compensation monocations associated with the anionic DNA backbone is established.[8b] Relatively high concentrations of $[Ru(NH_3)_6]^{3+}$ (5.0 μM) were used to shorten the time for equilibration. Representative voltammograms recorded under these conditions are shown in Figure 4-2A (red line).

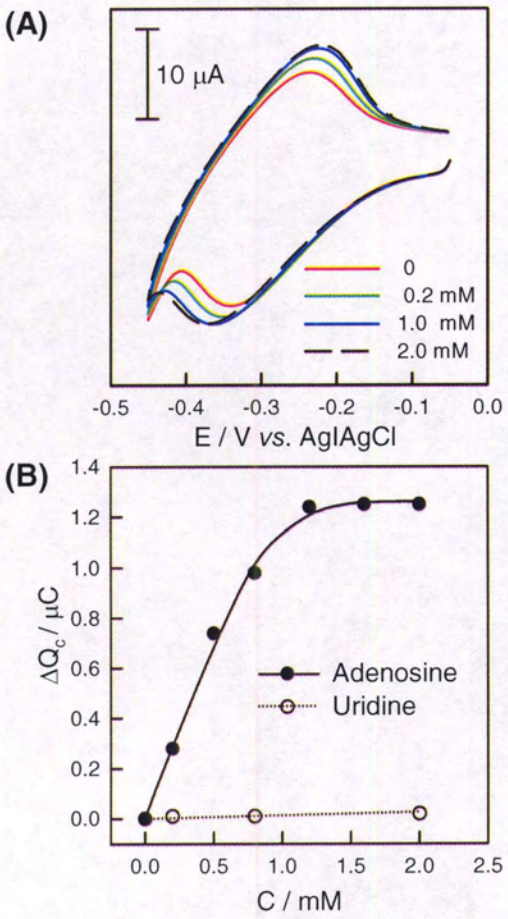

Figure 4-2 **(A) Cyclic voltammograms (CVs) of 5.0 μM $[Ru(NH_3)_6]^{3+}$ on a gold electrode modified with an adenosine-deoxyribosensor monolayer. The concentration of adenosine increased from 0 to 2 mM gradually. The scan rate was 300 mV/s. (B) Changes of the integrated charge (cathodic peaks) from the above CVs as function of concentration of adenosine (closed circle). Uridine (open circle) was used for the purpose of control experiments.**

The most striking observation in this study is the effect of adding adenosine to the electrolyte: both anodic and cathodic peak currents increase upon increasing the concentration of adenosine in solution. The dashed curve shows the steady-state CV recorded after adding a relatively high concentration (2.0 mM) of adenosine (beyond which no further changes were observed).

As described in our previous reports,[8] the surface-confined quantity of $[Ru(NH_3)_6]^{3+}$ ($\Gamma_{Ru\cdot DNA/Au}$) can be determined from the saturated charge (Q_{sat}) obtained by integration of the cathodic peak in the CVs (eq. 1).

$$Q_{sat} = nFA\Gamma_{Ru\cdot DNA/Au} \qquad (1)$$

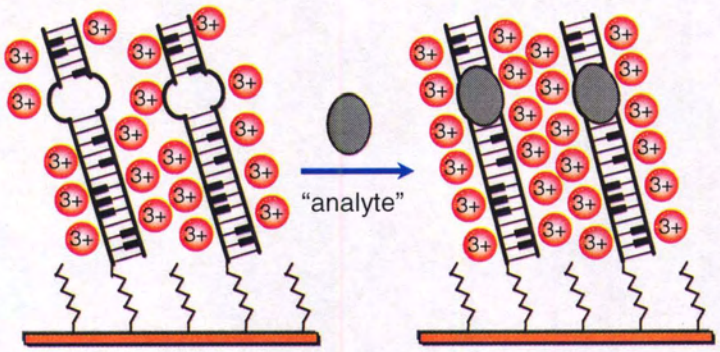

Figure 4-3 Schematic representation of the deoxyribosensor-modified gold electrode before and after binding with the analyte (adenosine) , with the presence of $[Ru(NH_3)_6]^{3+}$ in solution.

Figure 4-2B shows the dependence of the charge increase (ΔQ) on the concentration of adenosine in the electrolyte solution. Uridine, a nucleoside like adenosine, but with no affinity for binding this aptamer,[3] was used as a control to confirm that the increase of the charge resulted from the ligand-aptamer binding.[6]

We believe that the folding and compaction of the DNA aptamers induced by the binding of adenosine likely increased the negative charge density of the deoxyribosensors, with consequent binding of more $[Ru(NH_3)_6]^{3+}$ cations by electrostatic interaction (as illustrated in Figure 4-3), which in turn was reflected in the increased cyclic voltammetry peak area. By contrast, no significant changes were observed when uridine was added (Figure 4-4)

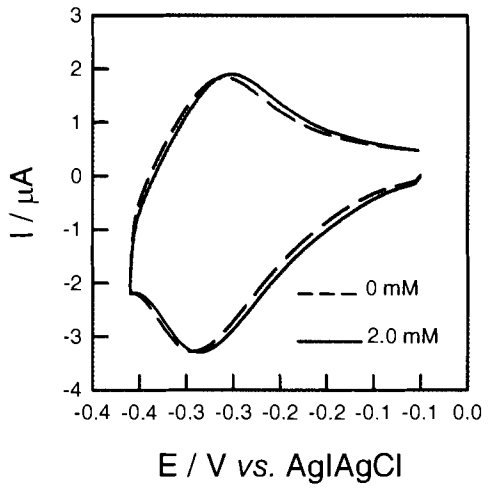

Figure 4-4 **Cyclic voltammograms of 5.0 μM $[Ru(NH_3)_6]^{3+}$ on deoxyribosensor-modified gold electrode without (solid line) and in the presence of 2.0 mM uridine (dotted line). The scan rate is 50 mV/s. No significant change in the integrated charge (peak area) was observed, rather than a small shift of the peak position.**

In addition to the selective sensing of adenosine, as illustrated in Figure 4-2, the equilibrium binding constant of adenosine to the surface-bound deoxyribosensors could be derived from the Langmuir model[8a,11b]

$$\frac{C}{\Delta Q_{eq}} = \frac{C}{\Delta Q_{sat}} + \frac{1}{K \cdot \Delta Q_{sat}} \qquad (2)$$

where $\Delta Q_{eq} = Q_{int} - Q_t$ and $\Delta Q_{sat} = Q_{int} - Q_{fin}$, Q_{int} is the saturated charge of $[Ru(NH_3)_6]^{3+}$ before adding adenosine, Q_t is the equilibrium charge of $[Ru(NH_3)_6]^{3+}$ after adding a certain concentration of adenosine, and Q_{fin} is the steady-state charge (in the presence of 2.0 mM adenosine). Figure 4-5 shows the linearized plot of the Langmuir isotherm for adenosine binding to the deoxyribosensor-modified gold electrode. The calculated binding constant K equals $(2.5\pm0.5) \times 10^3$ M^{-1}.

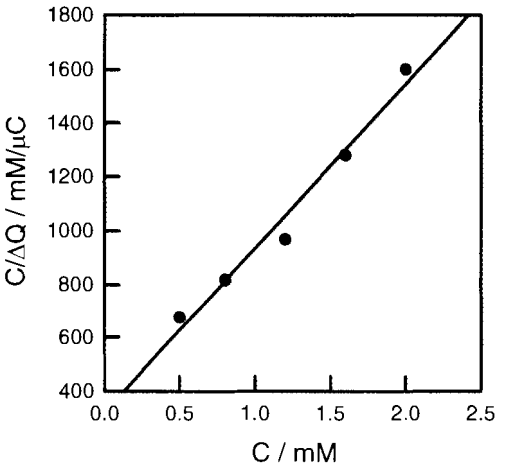

Figure 4-5 Linearized adsorption isotherms of $[Ru(NH_3)_6]^{3+}$ on the aptamer modified gold electrodes in terms of concentration of adenosine based on the Langmuir model.

This experiment represents our first step in exploring the direct electrical detection of biomedical analytes using deoxyribosensor chips. We note that the present method may not be the most optimally sensitive, given that it relies on a moderate increase of charge signal over a relatively high background. Currently, we are examining

the covalent attachment of electroactive labels to the deoxyribosensors to directly monitor charge transport from the redox centers to the electrode by way of the recognition moiety (aptamer).

4.2 Experimental Section

Detailed experimental procedures for the purification, hybridization process, surface-immobilization of synthetic DNA strands, have been reported previously (see chapter 2). The major difference is the sequences of the oligonucleotides used. To form the ATP aptamer, six mismatch bases are included in the design of the oligonucleotides, which are shown as underlined below.

The single strand oligonucleotide, 5'TTTAGCCAGGAGGAACCTTGAT3' and the disulfide derivative of the other strand, DMT-O-$(CH_2)_6$-S-S-$(CH_2)_6$-O-5'ATCAAGGTGGGGGATGGCTAAA3', were both purchased from Core DNA Services Inc. (Calgary, AB). Electrochemical measurements were performed in the same way as described in Chapter 2 and 3.

4.3 References

1. Gold, L.; Polisky, B.; Uhlenbeck, O.; Yarus, M. *Annu. Rev. Biochem.* **1995**, *64*, 763-797.
2. Herman, T.; Patel, D. J. *Science* **2000**, *287*, 820-825.
3. Huizenga, D. E.; Szostak, J. W. *Biochemistry* **1995**, *34*, 656-665.
4. Lin, C. H.; Patel, D. J. *Chem. Biol.* **1997**, *4*, 817-832.
5. For examples, see: (a) Giese, B.; Spichty, M. *Chem. Phys. Chem.* **2000**, *1*, 195-198. (b) Schuster, G. B. *Acc. Chem. Res.* **2000**, *33*, 253-260. (c) Boon, E. M.; Barton, J. K. *Curr. Opin. Strut. Bio.* **2002**, *12*, 320-329.
6. Fahlman, R. P.; Sen, D. *J. Am. Chem. Soc.* **2002**, *124*, 4610-4616.

7. (a) Merino, E. J.; Weeks, K. M. *J. Am. Chem. Soc.* **2003**, *125*, 12370-12371. (b) Pavlov, V.; Xiao, Y.; Shiyabovsky, B.; Willner, I. *J. Am. Chem. Soc.* **2004**, *126*, 11768-11769. (c) Ho, H.-A.; Leclerc, M. *J. Am. Chem. Soc.* **2004**, *126*, 1384-1387.

8. (a) Yu, H. Z.; Luo, C. Y.; Sankar, C. G.; Sen, D. *Anal. Chem.* **2003,** *75*, 3902-3907. (b) Su, L.; Sankar, C. G.; Sen, D.; Yu, H. Z. *Anal. Chem.* **2004,** *76*, 5953-5959.

9. For recent reviews of electrochemical DNA sensors, see (a) Drummond, T. G.; Hill, M. G.; Barton, J. K. *Nat. Biotechnol.* **2003**, *21*, 1192-1199. (b) Vercoutere, W.; Akeson, M. *Curr. Opin. Chem. Biol.* **2002**, *6*, 816-822. (c) Fojta, M. *Electroanalysis* **2002**, *14*, 1449-1463. (d) Wang, J. *Anal. Chim. Acta.* **2002**, *469*, 63-71.

10. For examples, see (a) Kelley, S. O.; Jackson, N. M.; Hill, M. G.; Barton, J. K. *Angew. Chem., Int. Ed.* **1999**, *38*, 941-945. (b) Yu, C. J.; Wan, Y. J.; Yowanto, H.; Li, J.; Tao, C. L.; James, M. D.; Tan, C. L.; Blackburn, G. F.; Meade, T. J. *J. Am. Chem. Soc.* **2001**, *123*, 11155-11161; (c) Patolsky, F.; Weizmann, Y.; Willner, I. *J. Am. Chem. Soc.* **2002**, *124*, 770-772. (d) Gore, M. R.; Szalai, V. A.; Ropp, P. A.; Yang, I. V.; Silverman, J. S.; Thorp, H. H. *Anal. Chem.* **2003**, *75*, 6586-6592. (e) Kim, E.; Kim, K.; Yang, H.; Kim, Y. T.; Kwak, J.; *Anal. Chem.* **2003**, *75*, 5665-5672.

11. (a) Steel, A. B.; Herne, T. M.; Tarlov, M. J. *Anal. Chem.* **1998,** *70*, 4670-4677. (b) Steel, A. B.; Herne, T. M.; Tarlov, M. J. *Bioconjugate Chem.* **1999,** *10*, 419-423.

CHAPTER 5
CONCLUDING REMARKS AND FUTURE WORK

In summary, this thesis described our electrochemical studies of metal ion-DNA interaction on surfaces, and explored sensing applications of DNA-modified electrodes. This augments the feasibility of direct electrochemical/electrical detection protocol in DNA sensing technology.

Firstly, the simple voltammetric procedure was extended to study the kinetics of metal ion-DNA interactions on surfaces. In particular, rate constants of $[Ru(NH_3)_6]^{3+}$ binding to and dissociation from DNA-modified surfaces were obtained by analyzing its time-dependent voltammetric behavior. It has been found that the binding kinetics are dominated by the structural nature of the DNA monolayer, i.e., the apparent first-order rate constant (k_{app}) decreases significantly upon increasing the surface density of DNA strands. The relatively slow kinetics are due to the compact structure of thiolate-DNA monolayers formed on gold.

It has been demonstrated that this method can be also used for the quantitative analysis of non-electroactive ions, specifically mono- and divalent metal cations of biological relevance (Mg^{2+}, Ca^{2+}, K^{+}), based on their competitive binding with $[Ru(NH_3)_6]^{3+}$ to DNA-modified surfaces. The sensitivity for dications (Mg^{2+} and Ca^{2+}) can reach a concentration as low as a few micromolar (μM). In addition, we were able to derive the equilibrium binding constants of Mg^{2+} and Ca^{2+} to DNA-modified electrodes base on the Langmuir model.

The first experiment to explore the feasibility of electrochemical deoxyribosensors for specific detection of molecular analytes was carried out. DNA assemblies incorporating an ATP/adenosine aptamer and a thiol-modifier were successfully immobilized onto gold electrode surface through sulfur-gold linkage. It has been shown that in the presence of analyte (adenosine), the switching to a 'ON' state can be detected directly by an increase of the cyclic voltammetric signals of pre-bound redox cations $[Ru(NH_3)_6]^{3+}$.

In the future, based on the idea described in chapter 3, the quantitative analysis of other types of cations, such as spermine that is of particular biological importance, can be explored. The cationic linear multivalent polyamine spermine $\{[(CH_2)_4(NH_2(CH_2)_3\text{-}NH_3)_2]^{4+}\}$ (Spm) is abundant in living cells and plays a key role in the structure, stabilization, and function of nucleic acids, due to the charge neutralization by the positively charged amino groups. Polyamines are essentially different from inorganic ions because they have no clear solvation shell. However, spermine may occupy DNA regions similar to magnesium and they may replace each other on the same sequence. Therefore, it should be interesting to study the binding thermodynamic/kinetics of spermine to DNA-modified surfaces based on its competitive binding with redox active cations.

Other sensing applications based on the electrochemical protocol could also be explored, such as detecting single base mismatch in a DNA double helix with the help of MutS, a mismatch binding protein. A thiolate DNA strand containing a single nucleotide mismatch could be immobilized on the gold surface. Upon exposing the sample to an electrolyte solution containing $[Ru(NH_3)_6]^{3+}$ until reaching equilibration, a steady cyclic voltammetric response from $[Ru(NH_3)_6]^{3+}$ could be detected. By adding MutS to the

electrolyte, the voltammetric signal should be decreased significantly, due to the binding of comparably big size MutS protein to the mismatched DNA strand.

As mentioned at the end of chapter 4, this is only our first step to explore the direct electrical detection of biomedical analytes by using deoxyribosensor chips. Future work on the development of novel deoxyribosensors will focus on the optimization of the detection protocols as well as design of novel DNA assemblies for specific sensing of certain type of molecular analytes. For example, redox-active group labeling of DNA has recently received much interest, as it provides direct current/charge signal. Covalent attachment of electroactive labels, such as the ferrocenoyl (Fc) group, to the deoxyribosensors to directly monitor charge transport from the redox centers to the electrode by way of the recognition moiety (apatmer) should be explored as our next milestone of success.